

Dear Editor,  
Dear Delphine Farmer

We would like to thank the two anonymous reviewers, which with their valuable comments and suggestions helped to further improve the manuscript.

Please find enclosed a document pointing to the specific minor and technical revisions addressed by the two referees.

In addition, we attach a marked-up manuscript version highlighting all changes made.

With kind regards, on behalf of all co-authors,

Armin Hansel & Werner Jud

## **Anonymous Referee #1**

### **Major comments**

**1. Figure 3 would benefit, if available, of data with ozone fumigation under dark condition in order to appreciate total ozone flux variation in the transition from light to dark conditions.**

*Author's response:* Figure 3 shows the transition from dark to light, but not from light to dark as in general our plant measurements were stopped while the plant was still illuminated. Therefore a plot showing both dark to light and light to dark transitions during ozone fumigation is not available. However Fig. S2 in the supplement shows ozone levels measured at the plant enclosure outlet, which are proportional to total ozone flux, during a light to dark transition in an experiment simulating diurnal ozone variations. We added a sentence in the caption of Fig. S2 explicitly mentioning the proportionality of the ozone flux.

**2. Statistics are needed in figure 4 in order to establish if differences between tobacco varieties are statistically significant.**

*Author's response:* Following the comment by reviewer #1, tobacco varieties and differences between light- and dark conditions were tested for statistical significance applying a Wilcoxon-Mann-Whitney test. This information was added to Fig. 4. A "Statistical analysis" section was added to the Methods section. Overall the outcome of the statistics supports the results already discussed in the manuscript.

## **Anonymous Referee #2**

**1. Since the authors acknowledged that the ozone surface reactions cannot be a defense mechanism, but instead is an "opportunistic ... side effect", the paper's title needs to be changed accordingly.**

*Author's response:* The title of the paper was changed as suggested to "Plant surface reactions: an opportunistic ozone defence mechanism impacting atmospheric chemistry"

**2. Much of the shown plant responses in terms of deposition of ozone and emissions of volatiles is qualitative. A calculation should be shown demonstrating the quantitative relationship between ozone loss and volatiles production, which, in turn, should allow statements about stomatal ozone losses beyond the qualitative ones made. If this calculation does significantly differ from what is shown in Figure 4, that needs to be explained.**

*Author's response:* The yields of volatile carbonyls were in the low percentage range. This is explained in the new section 3.5.

**3. Alongside such a calculation, another sample calculation should be presented comparing the "new" surface loss concept to the "old" one, thus demonstrating quantitatively the changes to stomatal ozone flux to be expected for plant species exhibiting an effective surface loss reaction.**

*Author's response:* These calculations are now presented in the new section 7 of the Supplement.

**4. In comparing Figures 3 and 4, it appears that virtually no effect was observed during the dark to light transition shown in Fig. 3, but displayed in Fig. 4. Explain.**

*Author's response:* During dark conditions the total ozone flux  $F_{\text{tot}}$  consists mainly of non-stomatal parts ( $F_{\text{ns}}$ ), while during light conditions  $F_{\text{tot}}$  equals the sum of nonstomatal ( $F_{\text{ns}}$ ) and stomatal ( $F_{\text{s}}$ )

fluxes. As we mention in the Methods part, the ozone concentration at the plant enclosure inlet was typically kept constant throughout an experiment. Therefore, the ozone concentration within the plant enclosure declined when stomatal ozone loss increased after starting plant illumination. Since fluxes depend on the ambient ozone concentration (see e.g. Supplement, section 7 ),  $F_{ns}$  dropped after dark to light transitions in experiments with tobacco varieties having a reactive leaf surface, while the total ozone flux  $F_{tot}$  slightly increased. This is why we used ozone conductances, which “normalize” fluxes with ozone concentrations, instead of ozone fluxes to show differences between different plant types or between the same plant type under light or dark conditions.

***5. I am having reservations with respect to the extrapolation arguments and speculation made in section 3.7; it appears somewhat selective in the sense of trying to find results supportive of the argument. For instance, the knowledge that pine needles contain high amounts of terpenes is not the same as those terpenes being secreted onto the surfaces of the needles (they are not). A main finding of the work is that ozone is only effectively deposited to a reactive surface that shows an obvious exposure to the atmosphere, and that condition is less widely found than the authors' new text suggests.***

***I suggest therefore to consider a few more works, including e.g. the Wolfe et al. CAFE papers and other papers that cite Holzinger et al., 2005.***

*Author's response:* We rewrote this paragraph and cited the suggested papers.

# Plant surface reactions: an opportunistic ozone defence mechanism impacting atmospheric chemistry

W. Jud<sup>1</sup>, L. Fischer<sup>1</sup>, E. Canaval<sup>1</sup>, G. Wohlfahrt<sup>2,3</sup>, A. Tissier<sup>4</sup>, and A. Hansel<sup>1</sup>

<sup>1</sup>Institute of Ion and Applied Physics, University of Innsbruck, 6020 Innsbruck, Austria

<sup>2</sup>Institute of Ecology, University of Innsbruck, 6020 Innsbruck, Austria

<sup>3</sup>European Academy of Bolzano, 39100 Bolzano, Italy

<sup>4</sup>Leibniz Institute of Plant Biochemistry, Department of Cell and Metabolic Biology, 06120 Halle, Germany

Correspondence to: A. Hansel (armin.hansel@uibk.ac.at)

**Abstract.** Elevated tropospheric ozone concentrations are considered a toxic threat to plants, responsible for global crop losses with associated economic costs of several billion dollars per year. Plant injuries have been linked to the uptake of ozone through stomatal pores and oxidative damage of the internal leaf tissue. But a striking question remains: can surface reactions limit the stomatal uptake of ozone and therefore reduce its detrimental effects to plants?

In this laboratory study we could show that semi-volatile organic compounds exuded by the glandular trichomes of different *Nicotiana tabacum* varieties are an efficient ozone sink at the plant surface. In our experiments, different diterpenoid compounds were responsible for a strongly variety dependent ozone uptake of plants under dark conditions, when stomatal pores are almost closed. Surface reactions of ozone were accompanied by a prompt release of oxygenated volatile organic compounds, which could be linked to the corresponding precursor compounds: ozonolysis of *cis*-abienol (C<sub>20</sub>H<sub>34</sub>O) – a diterpenoid with two exocyclic double bonds – caused emissions of formaldehyde (HCHO) and methyl vinyl ketone (C<sub>4</sub>H<sub>6</sub>O). The ring-structured cembratrien-diols (C<sub>20</sub>H<sub>34</sub>O<sub>2</sub>) with three endocyclic double bonds need at least two ozonolysis steps to form volatile carbonyls such as 4-oxopentanal (C<sub>5</sub>H<sub>8</sub>O<sub>2</sub>), which we could observe in the gas phase, too.

Fluid dynamic calculations were used to model ozone distribution in the diffusion limited leaf boundary layer under daylight conditions. In the case of an ozone-reactive leaf surface, ozone gradients in the vicinity of stomatal pores are changed in such a way, that the ozone flux through the open stomata is strongly reduced.

Our results show that unsaturated semi-volatile compounds at the plant surface should be considered as a source of oxygenated volatile organic compounds, impacting gas phase chemistry, as well as efficient ozone sink improving the ozone tolerance of plants.

## 1 Introduction

Tropospheric ozone ( $O_3$ ) is formed as a product of photochemical reactions involving nitrogen oxides ( $NO_x$ ) and volatile organic compounds (VOC) as precursors (Jenkin and Clemitshaw, 2000).  
25 Increasing anthropogenic precursor emissions from fossil fuel and biomass burning have led to elevated ambient ozone concentrations over large portions of the earth's surface. Today, many regions experience near-ground ozone background levels greater than 40 parts per billion volume (ppbv) (Vingarzan, 2004), levels which may be responsible for cellular damage inside leaves (Hewitt et al.,  
30 1990; Wohlgemuth et al., 2002) adversely affecting photosynthesis and plant growth (Ashmore, 2005). Toxic ozone concentrations cause visible leaf injury, plant damage and reduction in crop yields with associated economic costs of several billion dollars per annum worldwide (Wang and Mauzerall, 2004; Van Dingenen et al., 2009). Future trends of tropospheric ozone strongly depend on the emission factors of the corresponding precursor compounds (i.e. VOC and  $NO_x$ ) and indirectly also on land cover and characteristics of the vegetation (Dentener et al., 2006; IPCC, 2013; Fu and Tai, 2015). Some recent studies revealed a stabilization or even a lowering of the tropospheric background ozone concentrations in parts of the industrialized western countries since the turn of the millennium (Logan et al., 2012; Parrish et al., 2012; Oltmans et al., 2013; IPCC, 2013). This is likely a result of preventive measures reducing ozone precursor emissions (Granier et al., 2011).  
40 In contrast, ozone background concentrations are still rising in parts of Asia experiencing high economic growth and a concomitant increase in  $NO_x$  emissions (Granier et al., 2011; Fu and Tai, 2015). Land cover and land use changes, often determined by changing climatic conditions, could impact tropospheric ozone in different ways: A higher leaf area index of the vegetation would enhance dry deposition of ozone (Fu and Tai, 2015). In low  $NO_x$  regions enhanced emissions of isoprene emitting species could decrease ozone concentrations, while they would lead to an ozone increase in high  
45  $NO_x$  regions (Fu and Tai, 2015).

Traditionally, the risk of ozone damage to plants is estimated on the basis of the accumulated ozone exposure above 40 ppbv (AOT 40) (Felzer et al., 2005). However, the negative effects of ozone on vegetation have been observed to be more closely related to the effective dose, i.e. the  
50 stomatal flux  $\times$  time minus the portion of ozone which can be detoxicated by the plant defence system (Massman, 2004). In the expected  $CO_2$  richer and warmer future atmosphere (IPCC, 2013), plants may reduce stomatal conductance and thus indirectly alleviate ozone damage (Sitch et al., 2007).

However, accurate experimental quantification of the stomatal uptake of ozone is complicated by  
55 the presence of other ozone sinks, either in the gas phase or on the plant surface (Fruekilde et al., 1998; Cape et al., 2009). In previous studies the ozone flux through the stomata was calculated by multiplying the stomatal ozone conductance with the ambient ozone concentration (see e.g. Kurpius and Goldstein, 2003; Cieslik, 2004; Goldstein et al., 2004; Fares et al., 2012), assuming similar gradient profiles of ozone and  $H_2O$  close to the stomata. As we will show, for ozone-reactive leaf

60 surfaces this approach is not fully correct and may lead to an overestimation of stomatal ozone uptake in the case of very reactive surfaces.

We present results from ozone fumigation experiments, in which intact leaves of different varieties of tobacco (*Nicotiana tabacum*) were exposed to elevated ozone levels (20–150 ppbv) under light and dark conditions in an exceptionally clean plant enclosure system (see Materials and methods  
65 section for experimental details). The *Nicotiana tabacum* species is famous for large differences in the ozone tolerance of the different varieties. For example, the *Bel W3* is known to be very ozone sensitive (Heggstad, 1991; Loreto et al., 2001) and has therefore been used as an ozone indicator plant in earlier times (see Heggstad, 1991, and references therein). Conversely, the *Bel B* variety is known to be non-sensitive (Heggstad, 1991). The high ozone tolerance of this variety has been  
70 attributed to wider epidermal cells and more spongy mesophyll cell layers (Borowiak et al., 2010) and to differences in the plant's ability to cope with oxidative stress once ozone has entered the stomata (Schraudner et al., 1998; Eltayeb et al., 2007).

Several studies were investigating the possibility to increase the ozone tolerance of plants by external application of ozone-scavenging compounds (Gilbert et al., 1977; Loreto et al., 2001; Vickers et al.,  
75 2009a; Singh and Agrawal, 2010; Agathokleous et al., 2014) or by enabling the emission of volatile terpenoids in transgenic plants (Vickers et al., 2009b; Palmer-Young et al., 2015). We show here that some of the tobacco varieties investigated in our experiments are intrinsically equipped with ozone scavenging compounds located on their leaf cuticula. As is the case for many other plant species (Fahn, 1988), tobacco leaves possess glandular trichomes. In tobacco, various diterpenoids  
80 are the major compounds exuded by these secretory structures at the leaf surface (Sallaud et al., 2012). The exudates cover the plant leaves as a defence barrier, for example against arthropod pests (Wagner, 1991; Lin and Wagner, 1994); they were shown to have an anti-fungal (Kennedy et al., 1992) and insecticidal action (Kennedy et al., 1995). We show that in a tobacco variety secreting the diterpenoid *cis*-abienol, the exudates have a beneficial side-effect: they act as a powerful chemical  
85 protection shield against stomatal ozone uptake by depleting ozone at the leaf surface.

Surface-assisted ozonolysis not only protects plants from uptake of phytotoxic ozone through stomata, but also acts as a source of volatile carbonyls into the atmosphere, impacting atmospheric chemistry. To our knowledge, our study reports for the first time on detailed measurements of plant surface-assisted ozonolysis of semi-volatile diterpenoids forming volatile carbonyl products.

## 90 **2 Materials and methods**

### **2.1 Plant material**

We used the following four tobacco cultivars: *Ambalema*, secreting only the diterpenoid *cis*-abienol ( $C_{20}H_{34}O$ , see Fig. 1), *BYBA* secreting  $\alpha$ - and  $\beta$ -cembratrien-diols (CBTdiols,  $C_{20}H_{34}O_2$ , see

Fig. 1) and *Basma Drama*, secreting all these compounds (Sallaud et al., 2012). The new 3H02  
95 line does not exude diterpenoids at all (see Appendix A).

Seeds of the tobacco cultivars were obtained from the Leibniz Institute of Plant Biochemistry,  
Department of Cell and Metabolic Biology, Halle. The plants were grown in the green houses of the  
Institute of Ecology of the University of Innsbruck for 8–10 weeks in standard soil.

100 Before being used in the experiments the sample plants were allowed to adapt 1–4 weeks in the  
laboratory, obtaining light from the same true light lamp type as used during the measurements (see  
Setup section).

Plants were installed into the plant enclosure used for ozone fumigation the evening before the  
actual experiment, so they could adapt to the system and recover from possible stress during in-  
stallation. The sample plants were well watered and in a good physiological condition and showed  
105 no visible signs of damage. At the beginning of the experiments, when no ozone was added, no  
significant stress signals in form of green leaf volatiles were detected.

In total, combined dark and light ozone fumigation experiments were conducted with five *Ambalema*,  
two *Basma Drama*, one *BYBA* and three 3H02 samples. Moreover, experiments under solely  
light conditions were conducted with eight *Ambalema*, four *Basma Drama*, four *BYBA* and two 3H02  
110 plants. Each sample plant was tested only once.

## 2.2 Setup

In the present ozone experiments we used only inert materials such as Teflon<sup>®</sup>, PEEK<sup>®</sup> or Duran<sup>®</sup>  
glass in order to minimise artificial side-reactions of ozone with unsaturated compounds, present  
in e.g. sealing materials like rubber. Moreover, special care was taken to avoid fingerprints, which  
115 could result in side reactions of ozone with skin oils (Wisthaler and Weschler, 2010). Ozone loss,  
estimated from measured ozone concentrations at the inlet and outlet of the empty plant enclosure,  
was typically less than 5%.

For plant fumigation, synthetic air 5.0 grade was mixed with CO<sub>2</sub> 4.8 grade (both Messer Aus-  
tria GmbH, Gumpoldskirchen, Austria). By bubbling the air in distilled water and passing it by  
120 a subsequent thermoelectric cooler (TEC) the relative humidity was set. Before entering the plant  
enclosure, the air was flushed through an ozone generator (UVP, Upland (CA), USA). The enclosure  
system consisted of a desiccator (Schott Duran<sup>®</sup>) of 17.3 L volume, turned upside-down, and two  
end-matched PTFE<sup>®</sup> ground plates. A central hole served as feed-through for the plant stem, pos-  
sible gaps were sealed with Teflon<sup>®</sup> tape. The (single-sided) leaf area enclosed was typically in the  
125 range of 250–850 cm<sup>2</sup>.

An ozone detector (Model 49i, Thermo Fisher Scientific Inc. Franklin (MA), USA) and an infra-  
red gas analyser (LI-840A CO<sub>2</sub>/H<sub>2</sub>O Analyzer, LI-COR<sup>®</sup> inc., Lincoln (NE), USA) were sampling  
at 2 min intervals from either the inlet or outlet of the enclosure. Plant enclosure inlet ozone concen-  
trations were typically kept constant throughout each experiment and were adjusted to obtain real-

130 istic ambient ozone concentrations at the enclosure outlet during light conditions (e.g.  $\sim 60$  ppbv in Fig. 3). Relative humidity in the plant enclosure ranged from typically  $\sim 55\%$  in dark experiments up to  $\sim 95\%$  in light experiments.

VOC were quantitatively detected at the enclosure outlet by a Selective Reagent Ionization Time-of-Flight Mass Spectrometer (SRI-ToF-MS, see next section) which was switched every 6 min between  $\text{H}_3\text{O}^+$  and  $\text{NO}^+$  reagent ion mode.

140 Sample plants were illuminated by a true light lamp (Dakar, MT/HQI-T/D, Lanzini Illuminazione, Brescia, Italy). Infra-red light was shielded off by a continuously flushed water bath in order to prevent heating of the plant enclosure. Photosynthetically active radiation (PAR) was measured with a sunshine sensor (model BF3, Delta T Devices Ltd, Cambridge, UK) and temperature on the outer plant enclosure surface with K-type thermocouples.

### 2.3 SRI-ToF-MS

The UIBK Advanced SRI-ToF-MS (University of Innsbruck Advanced Selective Reagent Ionization Time-of-Flight Mass Spectrometer, Breitenlechner and Hansel, 2015) combines the high mass resolution of PTR-ToF-MS (Graus et al., 2010) with the capability to separate isomeric compounds having specific functional groups. For this purpose, the SRI-ToF-MS makes use of different chemical ionization pathways of a set of fast switchable primary ions (here:  $\text{H}_3\text{O}^+$  and  $\text{NO}^+$ ). Moreover, the employment of different primary ions could help to differentiate molecules suffering from fragmentation onto the same mass to charge ratio in the standard  $\text{H}_3\text{O}^+$  mode (Karl et al., 2012).

150 Examples of differentiable isomers are aldehydes and ketones. In the  $\text{H}_3\text{O}^+$  reagent ion mode, aldehydes and ketones both exhibit proton transfer and thus e.g. methyl vinyl ketone (MVK) and methacrolein (MACR) are both detected as  $\text{C}_4\text{H}_7\text{O}^+$  ( $m/z$  71.050). In  $\text{NO}^+$  reagent ion mode, most aldehydes exhibit hydride ion transfer and ketones clustering reactions, comparable to the ionization mechanisms in a SIFT instrument (Španěl et al., 1997). Thus MVK is detected as  $\text{C}_4\text{H}_6\text{O} \cdot \text{NO}^+$  ( $m/z$  100.040), whereas MACR is detected as  $\text{C}_4\text{H}_5\text{O}^+$  ( $m/z$  69.034).

155 In addition to isomeric separation, the high flow through the drift tube (here:  $\sim 500 \text{ mL min}^{-1}$  compared to  $10\text{--}20 \text{ mL min}^{-1}$  in a standard instrument) allows for the first time the detection of semi-volatile compounds such as the diterpenoid *cis*-abienol ( $\text{C}_{20}\text{H}_{34}\text{O}$ ).

The SRI-ToF-MS was operated under standard conditions,  $60^\circ\text{C}$  drift tube temperature, 540 or 350 V drift voltage and 2.3 mbar drift pressure, corresponding to an  $E/N$  of 120 or 78 Td ( $E$  being the electric field strength and  $N$  the gas number density;  $1 \text{ Td} = 10^{-17} \text{ V cm}^2$ ) in  $\text{H}_3\text{O}^+$  or  $\text{NO}^+$  reagent ion mode, respectively. The instrument was calibrated approximately once a week by dynamic dilution of VOC using 2 different gas standards (Apel Riemer Environmental Inc., Broomfield (CO), USA), containing ca. 30 different VOC of different functionality distributed over the mass range of 30–204 amu. Full SRI-ToF-MS mass spectra were recorded up to  $m/z$  315 with a 1 s time



165 resolution. Raw data analysis was performed using the PTR-ToF Data Analyzer v3.36 and v4.17 (Müller et al., 2013).

## 2.4 *cis*-abienol identification

For the identification of *cis*-abienol a pure standard was acquired (Toronto Research Chemicals, Toronto, Canada). The powder was dissolved in n-hexane and applied on the surface of a glass  
170 container, which was put into the enclosure system and treated like the plant samples. In  $\text{H}_3\text{O}^+$  reagent ion mode, the major *cis*-abienol derived signal was detected on  $m/z$  273.258 ( $\text{C}_{20}\text{H}_{33}^+$ ); like many other alcohols, *cis*-abienol is losing  $\text{H}_2\text{O}$  after the protonation reaction. Minor fragment signals in the range of a few percent were detected at  $m/z$  191.180 ( $\text{C}_{14}\text{H}_{23}^+$ ),  $m/z$  163.149 ( $\text{C}_{12}\text{H}_{19}^+$ ) and  $m/z$  217.196 ( $\text{C}_{16}\text{H}_{25}^+$ ), respectively.

175 In  $\text{NO}^+$  reagent ion mode, the major *cis*-abienol derived signals were detected at  $m/z$  272.250 ( $\text{C}_{20}\text{H}_{32}^+$ ) and  $m/z$  178.172 ( $\text{C}_{13}\text{H}_{22}^+$ ). Minor signals were measured at  $m/z$  163.149 ( $\text{C}_{12}\text{H}_{19}^+$ ) and  $m/z$  134.101 ( $\text{C}_{10}\text{H}_{14}^+$ ), respectively.

Ozonolysis of the pure *cis*-abienol standard yielded the same primary ozonolysis products (see below) as in the case of *Ambalema* plants.

## 180 2.5 Leaf stripping

In order to relate the observed ozonolysis carbonyls to plant surface reactions, leaf exudates of untreated tobacco plants were stripped off by dipping leaves (of similar area) of untreated *Ambalema*, *Basma Drama* and 3H02 plants into n-hexane ( $\sim 100$  mL for  $1000\text{ cm}^2$  leaf area) for  $\sim 1$  min. The n-hexane – leaf exudate solution was then distributed as evenly as possible onto the inner surface of the  
185 empty desiccator serving as plant enclosure. n-hexane evaporated quickly and was further reduced by flushing the glass cuvette with pure synthetic air. Afterwards, ozone fumigation experiments were performed similar to the experiments with intact plants.

## 2.6 GC-MS analysis

Non-volatile ozonolysis products and unreacted surface compounds were analysed by GC-MS (see  
190 also Supplement). Directly after the ozone fumigation experiments we extracted leaf exudates and low volatility ozonolysis products from the fresh tobacco leaves (see Leaf Stripping section).  $1\ \mu\text{L}$  portions of the samples were then injected directly into a GC-MS for analysis on a 6890 N gas chromatograph coupled to a 5973 N mass spectrometer (Agilent Technologies) according to the procedures described elsewhere (Sallaud et al., 2012).

195 Tobacco diterpenoids were identified on the basis of their mass spectra, as described in the literature (Enzell et al., 1984).

## 2.7 Calculation of leaf gas exchange parameters

For the calculation of the gas exchange parameters we followed well established procedures by Caemmerer and Farquhar (1981) and Ball (1987). Transpiration rate  $E$ , assimilation rate  $A$ , total ozone flux  $F_{\text{tot},\text{O}_3}$  and total water vapour conductance  $g_{\text{l,H}_2\text{O}}$  were calculated from

$$E = \frac{u_e}{s} \cdot \frac{w_o - w_e}{1 - w_o \cdot 10^{-3}}, [\text{mmol m}^{-2} \text{s}^{-1}] \quad (1)$$

$$A = \frac{u_e}{s} \cdot \left[ c_e - \left( \frac{1 - w_e \cdot 10^{-3}}{1 - w_o \cdot 10^{-3}} \right) \cdot c_o \right], [\mu\text{mol m}^{-2} \text{s}^{-1}] \quad (2)$$

$$F_{\text{tot},\text{O}_3} = \frac{u_e}{s} \cdot \left[ o_e - \left( \frac{1 - w_e \cdot 10^{-3}}{1 - w_o \cdot 10^{-3}} \right) \cdot o_o \right], [\text{nmol m}^{-2} \text{s}^{-1}] \quad (3)$$

$$g_{\text{l,H}_2\text{O}} = \frac{10^3 \cdot E \left( 1 - \frac{w_o + w_i}{2 \cdot 10^3} \right)}{w_i - w_o}, [\text{mmol m}^{-2} \text{s}^{-1}] \quad (4)$$

with  $u_e$  the molar flow of air entering the enclosure in  $[\text{mol s}^{-1}]$ ,  $s$  the leaf area in  $[\text{m}^2]$ ,  $w_e/c_e/o_e$  and  $w_o/c_o/o_o$  the mole fraction of water vapour/ $\text{CO}_2$ /ozone entering respectively leaving the plant enclosure in  $[\text{mmol mol}^{-1}]$ ,  $[\mu\text{mol mol}^{-1}]$  and  $[\text{nmol mol}^{-1}]$ , respectively.  $w_i$  is the mole fraction of water vapour inside the leaf in  $[\text{mmol mol}^{-1}]$  and is typically assumed to be the saturation mole fraction at leaf temperature (Ball, 1987).

For the calculation of the total ozone conductance we applied a ternary diffusion model as has been proposed by Caemmerer and Farquhar (1981). Thereby, pairwise interactions between ozone, water vapour and air are considered (for the sake of simplicity we neglected interactions with  $\text{CO}_2$ ). Interactions of ozone molecules with water vapour are important only for that portion of ozone, which is entering the stomatal pores and not for that lost in reactions at the leaf surface. However, in the latter case the consideration of binary diffusion between ozone and water leads to an overestimation of the total ozone conductance in the range of  $< 1\%$ .

Total ozone conductance  $g_{\text{l},\text{O}_3}$  is then defined by

$$g_{\text{l},\text{O}_3} = \frac{-10^3 \cdot F_{\text{tot},\text{O}_3} + \left( \frac{o_a + o_i}{2} \right) \cdot E}{o_a - o_i}, [\text{mmol m}^{-2} \text{s}^{-1}] \quad (5)$$

with  $o_i$  and  $o_a$  the mole fractions of ozone inside the leaf (at the leaf surface for reactive leaf surfaces) and in the surrounding air, respectively.  $o_a$  equals the ozone mole fraction  $o_o$  measured at the outlet of the plant enclosure. Typically, we consider  $o_i \approx 0$  (Laisk et al., 1989) and therefore Eq. (5) simplifies further to

$$g_{\text{l},\text{O}_3} = \frac{-10^3 \cdot F_{\text{tot},\text{O}_3} + \frac{o_a}{2} \cdot E}{o_a} \quad (6)$$

## 2.8 Quantification of the ozone depletion capability of individual plants

In our fumigation experiments the ozone concentrations in the plant enclosure varied between the different experiments and within experiments switching from light to dark conditions. In order to compare the ozone depletion capability (i.e. surface plus stomatal sinks) of different plants or of

the same plant under dark and light conditions, it is therefore important to use a concentration independent measure. As for a given ozone conductance the ozone flux increases with the ambient  
230 ozone concentration (cf. Eqs. 3+6), we follow others (see e.g. Wohlfahrt et al., 2009) and use the ozone conductance values instead. In experiments with plants having an ozone reactive surface, the total ozone conductance  $g_{l,O_3}$  (Eq. 6) comprises boundary layer conductance, stomatal conductance and cuticular conductance. Stomatal and boundary layer ozone conductances can be calculated from those of water vapour by correcting for the different diffusivities of the two gases. The boundary  
235 layer water vapour conductance could be determined by measuring temperature and evaporation rate from leaf models made of chromatography paper (see Ball 1987). However, in our experiments this was not really practical for all sample plants which were all complexly and differently shaped. Consequently, also the stomatal water vapour and ozone conductances could not be inferred from the calculated total water vapour conductance (Eq. 4).

240 As we show in the Supplement, even if stomatal and boundary layer ozone conductances are known, for semi-reactive leaf surfaces the calculation of stomatal and non-stomatal parts of the total ozone flux is not feasible.

For these reasons we report here only total ozone conductance values (Eq. 6), normalized to the single-sided leaf area or to the area of the enclosure covered with leaf exudates in experiments with  
245 pure leaf surface compounds (see Sec. 2.5).

## 2.9 Statistical analysis

Data ( $g_{l,O_3}$ ,  $A$ ,  $g_{l,H_2O}$ ) were tested for statistically significant differences between dark and light experiments (using the same variety) and between different tobacco varieties (in either dark or light experiments), respectively, using the Wilcoxon-Mann-Whitney test in Matlab<sup>®</sup>. Due to the  
250 partially small sample size, probabilities  $p < 0.1$  are reported as marginally significant. Lacking replicates of dark experiments with *BYBA* plants, in the statistical analysis this type of experiments was omitted.

## 2.10 Fluid dynamic calculations

In order to visualise the ozone concentration gradients caused by plant ozone uptake, two idealised  
255 setups were simulated: a macroscopic plant model in an ambient air flow and a microscopic model for the stomatal gas exchange. The simulations were done using the open source CFD code OpenFOAM (www.openfoam.com).

In the microscopic model the air flow was neglected and a pure diffusion process was simulated. Stomata were modelled as 100  $\mu\text{m}$  long and 40  $\mu\text{m}$  wide eye-shaped openings recessed 20  $\mu\text{m}$  deep  
260 into the leaf surface. The simulation domain with 500 000 cells covered an area of 300  $\mu\text{m}$  square around the stoma and extended 2 mm from the leaf surface into the surrounding gas. A single stoma with cyclic boundaries was used to represent a whole leaf with stomata spread repeatedly over its

surface. The ozone-reactive bottom of the stomata was modelled as 100% efficient sink (Laisk et al., 1989) with a constant ozone concentration of zero, while the side walls of the stomata were assumed not to absorb ozone and set to zero gradient. The top of the measurement domain acting as ozone inlet from the surrounding was set to one. The leaf surface around the stomata was set to zero gradient or to a fixed concentration of zero, representing two idealised plant types with either non-reactive or reactive leaf surface. “scalarTransportFoam” was run on this grid with a uniform zero velocity field until a steady state was reached.

For the macroscopic model (see Supplement) a laminar flow around the plant was simulated using the steady state Reynolds averaged Navier–Stokes solver “simpleFoam”, the transport of ozone in the resulting flow velocity field was studied using the “scalarTransportFoam” solver. The simulated gas volume consisted of a cube with 20 cm edge length with the shape of an exemplary tobacco plant cut out of its volume (see Fig. S3). The resulting simulation domain was divided into a hexahedron-dominant grid of 3.7 million cells with the finest granularity around the stomata and the leaf surfaces with the OpenFOAM tool “snappyHexMesh”. The domain was divided into eight subdomains for parallel computation. Stomata were represented by small patches spread equally over the leaf surfaces, covering 10% of the total leaf area. The boundary conditions for the gas flow simulation consisted of an inlet with  $2 \text{ mm s}^{-1}$  velocity entering on one face of the cube and a constant pressure boundary condition outlet on the opposite face. The gas velocity on the plant surface was set to zero. Initial conditions for the flow simulation were calculated with “potentialFoam” to speed up convergence of the “simpleFoam” solver. The simulation was run until the flow velocity field reached a steady state. For the diffusion calculations a relative initial concentration of ozone was set to one at the inlet and to zero on the stomata patches. Like in the microscopic model calculations, the leaf surface was either a zero concentration gradient boundary (for an idealised 3H02 plant type) or a fixed concentration value of zero (for an idealised *Ambalema* plant type). In the previously calculated velocity field the ozone transport was simulated until a steady state was reached, too.

### 3 Results and discussion

#### 3.1 Expected ozonolysis products of *cis*-abienol and cembratrien-diols

Apart from the 3H02 variety, the investigated tobacco varieties secrete different unsaturated diterpenoids (see Sec. 2.1). According to the Criegee mechanism (Criegee, 1975), ozone attacks the carbon double bonds of alkenes forming primary carbonyls and so-called Criegee Intermediates (see Supplement). Criegee Intermediates are, however, expected to be too short-lived to be detected directly by the instruments used in our experiments (see Supplement). We were therefore interested primarily in the stable, volatile ozonolysis carbonyls, which could be detected in real-time by our SRI-ToF-MS.

For the semi-volatile diterpenoid *cis*-abienol with two exocyclic double bonds, exuded by the *Am-*

*balema* and *Basma Drama* varieties, we expected the formation of formaldehyde (HCHO) and methyl vinyl ketone (MVK, C<sub>4</sub>H<sub>6</sub>O, see Fig. 1).

300 In the case of the ring structured CBTdiols with three endocyclic double bonds, produced by the *Basma Drama* and *BYBA* plants, at least two ozonolysis steps are needed to form volatile carbonyls. The three smallest carbonyl products are shown in Fig. 1, whereby 4-oxopentanal (C<sub>5</sub>H<sub>8</sub>O<sub>2</sub>) is expected to be the most volatile one (Goldstein and Galbally, 2007).

### 3.2 Ozone fumigation experiments with pure leaf surface compounds

305 In order to relate a release of carbonyls to surface chemistry only and to exclude stimulated emissions caused, e.g. by the plant ozone defence system, we investigated ozone reactions with pure leaf surface extracts. Leaf surface compounds were extracted with n-hexane and subsequently applied onto the inner surface of an empty plant enclosure and fumigated with ozone (see Materials and methods section).

310 *Ambalema* leaf extracts showed a weak signal of *cis*- abienol (we refer to the Materials and methods section for the identification of this compound), which disappeared during ozone fumigation while MVK and formaldehyde were prominently observed. These carbonyls ~~are~~ **were** produced by surface-assisted ozonolysis of *cis*-abienol (see Fig. 1). MVK was detected at  $m/z$  71.050 (C<sub>4</sub>H<sub>7</sub>O<sup>+</sup>) and  $m/z$  100.040 (C<sub>4</sub>H<sub>6</sub>O • NO<sup>+</sup>) in the H<sub>3</sub>O<sup>+</sup> respectively NO<sup>+</sup> reagent ion mode of the SRI-ToF-  
315 MS. Formaldehyde was detected only using H<sub>3</sub>O<sup>+</sup> as reagent ion at  $m/z$  31.018 (CH<sub>3</sub>O<sup>+</sup>), taking into account the humidity dependent sensitivity (Hansel et al., 1997). In the NO<sup>+</sup> reagent ion mode formaldehyde cannot be ionized (Španěl et al., 1997), consequently we detected no signal.

In the ozone fumigation experiments using *Basma Drama* leaf extracts, besides MVK and formaldehyde as ozonolysis products of *cis*-abienol, also the most volatile CBTdiol ozonolysis product –  
320 4-oxopentanal – was detected in the gas phase by SRI-ToF-MS. 4-oxopentanal was detected at  $m/z$  101.060 (C<sub>5</sub>H<sub>9</sub>O<sub>2</sub><sup>+</sup>) in H<sub>3</sub>O<sup>+</sup> and  $m/z$  99.045 (C<sub>5</sub>H<sub>7</sub>O<sub>2</sub><sup>+</sup>) in NO<sup>+</sup> reagent ion mode, respectively.

No significant amount of volatile carbonyls was observed from ozonolysis of 3H02 leaf extracts. Consistently, the total ozone conductance was far less than in experiments with extracts from  
325 diterpenoid-exuding tobacco varieties (see Fig. 2). This is in line with the results from the corresponding experiments with intact plants (see below). The ozone depletion efficiency of the 3H02 exudates was decreasing fast, while the presence of *cis*-abienol in *Ambalema* leaf exudates kept the ozone conductance at elevated levels for many hours (cf. Fig. 2).

### 3.3 Ozone fumigation experiments with diterpenoid exuding tobacco varieties

330 Also in experiments with intact plants we observed a prompt release of volatile carbonyls as soon as the tobacco leaves were fumigated with ozone. The *Ambalema* and *Basma Drama* varieties released MVK and formaldehyde. In addition, we detected sclaral, a non-volatile compound, in surface ex-

tracts obtained from ozone fumigated plants of the same varieties (see Materials and methods and Supplement). Sclaral is an isomerisation product of the C<sub>16</sub> carbonyl formed in *cis*-abienol ozonolysis (cf. Fig. 1). All these compounds can therefore be attributed again to surface-assisted ozonolysis of *cis*-abienol (see Fig. 1).

In experiments using *Basma Drama* and *BYBA* plants we detected the CBTdiol ozonolysis product 4-oxopentanal, similar to the ozone fumigation experiments with leaf surface extracts (see previous section).

Figure 3 shows a typical result of an ozonolysis experiment using *Ambalema* plants. Immediately after starting the ozone fumigation, the *cis*-abienol signal decreased, while initial bursts of MVK and formaldehyde were detected. These initial bursts can be attributed to surface ozonolysis of *cis*-abienol deposited on *all* surfaces (i.e. surfaces of the whole plant, the enclosure and the enclosure outlet tubing) during plant acclimatisation under ozone free conditions lasting > 12h (see Sec. 3.6 and Supplement).

In plant experiments using diterpenoid exuding tobacco varieties, the carbonyl emission and consequently the total ozone conductance and flux (under constant light) eventually reached a steady state, when the diterpenoid production by the trichomes (leading to a permanent deposition of those onto the plant surface) and plant surface reactions were in equilibrium (cf. Fig. 3). This is in contrast to experiments with pure leaf surface compounds, in which the diterpenoids were slowly consumed as ozone fumigation progressed (see Sec. 3.2).

Simulating diurnal ozone variations over two days in experiments with *Ambalema* and *Basma Drama* plants, we could show that the reactive layer at the plant surface is a large pool and not quickly consumed (see Supplement and Fig. S2). We therefore assume that the diterpenoids released are likely to represent a long term ozone protection for these varieties.

### 3.4 Variety specific ozone depletion during dark and light phases

In further experiments we investigated the ozone depletion by different tobacco varieties under dark and light conditions.

In dark experiments, when stomatal pores are almost closed, the *Ambalema* variety showed the highest total ozone conductance under steady-state conditions (cf. Fig. 4a). This is a direct indication for the high ozone depletion capacity of the surface of this variety.

Due to the lack of reactive diterpenoids on the leaf surface of 3H02 plants, the surface ozone sink plays a minor role for this tobacco line. However, we cannot totally exclude the presence of other unsaturated compounds at the surface of this variety.

The low surface reactivity of the *Basma Drama* and *BYBA* varieties correlates with the lower amount of detected ozonolysis carbonyls compared to that of the *Ambalema* variety in dark conditions. This might be related to a lower diterpenoid surface coverage of these two varieties and the expected lower reactivity of the CBTdiols having endocyclic double bonds (Atkinson and Arey, 2003).

The *Ambalema* variety also shows a higher  $g_{1,H_2O}$  and dark respiration than the other varieties (cf. Fig. 4b+c).  $g_{1,H_2O}$  linearly correlates with the stomatal water vapour conductance and therefore also with the stomatal ozone conductance. However, higher stomatal conductance during dark conditions cannot explain the large differences in  $g_{1,O_3}$  between the plant types. While  $g_{1,H_2O}$  of the *Ambalema* variety in dark conditions is about twice as high as that of the 3H02 variety, the corresponding  $g_{1,O_3}$  is four times as high.

When switching from dark to light conditions we assume cuticular conductance not to change significantly and thus an increase in the calculated  $g_{1,O_3}$  is attributable mainly to an increasing stomatal ozone conductance. In the case of *Ambalema*, switching the light on increased the total conductance by  $\sim 55\%$  (see Fig. 4a). In contrast, in the 3H02 case, switching on the light triggered an substantial increase in the total ozone conductance by  $\sim 340\%$  (cf. Fig. 4a).

During light conditions the total ozone conductances of the different tobacco varieties were in a comparable range; slightly higher values were observed for the diterpenoid exuding lines *Ambalema*, *Basma Drama* and *BYBA*.

Statistical analysis confirmed the observed tendencies of the total ozone conductance: only for the *Ambalema* variety was  $g_{1,O_3}$  under light conditions not significantly different from the values measured under dark conditions ( $p > 0.1$ ). Conversely,  $g_{1,O_3}$  calculated for the *Ambalema* variety was significantly higher than that of the other tobacco lines under dark conditions ( $p < 0.1$ , see Fig. 4a).

### 3.5 Volatile carbonyl yields from surface ozonolysis

In the ozone fumigation experiments the yield of volatile ozonolysis products was generally in the low percentage range, e.g. for *Ambalema* plants  $\sim 7\%$  under dark and  $\sim 5\%$  under light conditions considering the major volatile ozonolysis products MVK and formaldehyde quantified by SRI-TOF-MS. The slight change from  $\sim 7\%$  to  $\sim 5\%$  when switching from dark to light conditions can be explained by the effect of the open stomata. Open stomata offer an alternative sink for ozone and for volatile carbonyls produced in surface assisted reactions (Karl et al., 2010; Niinemets et al., 2014). The reason why only a small percentage of the consumed ozone is detected as volatile products indicates that most of the ozonolysis products are not volatile enough to leave the plant surface (cf. Fig. 1 and Supplement). The fate of the Criegee Intermediates in surface ozonolysis is discussed in detail in the Supplement.

### 3.6 Separation of ozone surface and gas phase reactions

In order to qualify the measured total ozone fluxes for the calculation of  $g_{1,O_3}$  values, we had to take into account the possibility of homogeneous gas phase ozonolysis of the semi-volatile diterpenoids exuded by the tobacco varieties.

To assess the significance of gas phase ozonolysis to our results, we connected the plant enclosure

containing a diterpenoid emitting tobacco plant with a second empty enclosure downstream and  
405 added ozone only to the second enclosure. Only negligible carbonyl signals were observed once the  
initial burst from deposited diterpenoids faded away (see Supplement and Fig. S1). This result indi-  
cates that with our setup gas-phase reactions of the diterpenoids were not significant.

This observation can be explained theoretically, too. The air in our enclosure system was exchanged  
every  $\sim 5$  min. Therefore, only extremely fast gas phase ozone – alkene reactions have to be consid-  
410 ered. For an ozone concentration of 100 ppbv, a reaction rate of  $1.35 \times 10^{-15} \text{ cm}^3 \text{ s}^{-1}$  results in an  
alkene ozonolysis lifetime of 5 min. Such fast ozonolysis rates have only been measured for a few  
very reactive sesquiterpenes (Atkinson and Arey, 2003). We found no reaction rates of *cis*-abienol  
and CBTdiols with ozone in the literature to exclude the possibility of a gas phase contribution to  
total ozone loss in our experiments a priori. Nonetheless, taking into account the estimated vapour  
415 pressures of *cis*-abienol ( $\sim 10^{-9}$  bar) and CBTdiol ( $\sim 10^{-12}$  bar) (Goldstein and Galbally, 2007) we  
can state that the bulk of the exuded diterpenoids stayed at the leaf surface and that other surfaces  
(e.g. the inner surface of the plant enclosure and the tubing system) were very slowly covered by  
condensed diterpenoids. This is also the explanation for the bursts of volatile ozonolysis products  
at the beginning of every ozone fumigation (see e.g. Fig. 3). We therefore assume that gas phase  
420 reactions are unlikely to have played a major role in our experiments.

### 3.7 Fluid dynamic model calculations

Microscopic fluid dynamic model calculations (see Materials and methods) revealed the principles  
responsible for the strong variety-dependent partitioning between stomatal and non-stomatal ozone  
loss (see Sect. 3.4). The mixed convective and diffusive ozone transport from the surrounding atmo-  
425 sphere to the plant surface and into the stomata was simulated for two idealised plant types under  
light conditions when the leaf stomata are open. The stomatal pores were exemplarily modelled as  
small patches uniformly spread over the entire leaf surface. For one model plant we assumed stom-  
atal ozone uptake only, corresponding to an idealised 3H02 variety plant lacking any reactive surface  
compounds. The second model plant was representing an idealised *Ambalema* variety. The surface  
430 acted as a perfect ozone sink with every ozone molecule reaching it being lost, either on the leaf  
surface or through the stomata.

Figure 5a and b show the resistance schemes used to describe the ozone flux to the leaves in the two  
scenarios, which were the basis for our simulations. Ambient ozone has to overcome the boundary  
layer resistance  $R_b$  and the stomatal resistance  $R_s$  before being destroyed in the stomatal cavity (for  
435 the sake of simplicity we neglected here the **mesophyll mesophyll** resistance, which comprises diffusion  
through inner air spaces and dissolution of the gas in the cell wall water, followed by losses in  
the aqueous phase, penetration of plasmalemma or chemical reactions in the cell, cf. Neubert et al.,  
1993). In the case of a non-reactive leaf surface, ozone depletion within the stomata is the sole ozone  
sink (see Fig. 5a).



440 In the case of an ozone-reactive leaf surface, an additional surface chemical resistance  $R_{sc}$  has to be introduced, which is parallel to the stomatal resistance (see Fig. 5b).  $R_{sc}$  inversely correlates with the reactive uptake coefficient of ozone at the leaf surface. In the case of the model plant having a non-reactive surface,  $R_{sc}$  is very large ( $R_{sc} \rightarrow \infty$ ) and ozone flux to the leaf surface can be omitted. Conversely,  $R_{sc}$  is small for reactive surfaces.

445 The porous leaf surface architecture has special relevance for the gas uptake of plants. For gases having a negligible leaf surface sink (or source) – like e.g.  $\text{CO}_2$  – steep concentration gradients parallel and perpendicular to the surface develop in close proximity to the stomata. These gradients enhance the gas transport in the diffusive leaf boundary layer towards the pores. This effect is extensively described in the literature as the “paradox of pores” (see e.g. Monson and Baldocchi, 2014). It  
 450 enables plants to effectively harvest  $\text{CO}_2$  for photosynthesis, but in the same manner also “funnels” phytotoxic ozone through the stomata into the plant leaves (see Fig. 5c).

In the case of an ozone-reactive leaf surface,  $R_{sc}$  is small compared to  $R_s$  and only surface-parallel ozone concentration isosurfaces develop (black lines in Fig. 5d). Concentration gradients (white lines) close to the stomata are exclusively perpendicular to the surface. Consequently, the ozone  
 455 transport in the diffusive leaf boundary layer is equally distributed over the whole leaf surface and the ozone concentration in this layer is strongly reduced (see Fig. 5d). Similarly, also macroscopic model calculations show that this effect broadens the space of reduced ozone concentrations surrounding a plant with opened stomata (see Supplement and Fig. S3).

The surface-parallel concentration isosurfaces are the reason why we can use the same reference  
 460 concentration  $c_{b,r}$  for both the stomatal and the surface chemical resistance, (cf. Fig. 5b). However, this approach does only hold if the leaf surface is a complete ozone sink (see Supplement and Fig. s4S5).

The different ozone concentration patterns in the two modelled scenarios have important implications for the stomatal ozone uptake. Typically, the stomatal conductance of ozone  $g_{s,\text{O}_3}$  is estimated  
 465 from that of water  $g_{s,\text{H}_2\text{O}}$ , by correcting for the different diffusivity of the two gases (see e.g. Ball, 1987; Neubert et al., 1993). The stomatal ozone flux  $F_{s,\text{O}_3}$  can then be calculated with the following formula:

$$F_{s,\text{O}_3} = g_{s,\text{O}_3} \cdot (c_{i,\text{O}_3} - c_{b,\text{O}_3}) \quad (7)$$

with  $c_{i,\text{O}_3}$  being the ozone concentration in the leaf intercellular space and  $c_{b,\text{O}_3}$  the ozone concentration in the leaf boundary layer. For high ambient ozone concentrations  $c_{i,\text{O}_3}$  was found to be  
 470 positive (Moldau and Bichele, 2002; Loreto and Fares, 2007), but typically it is assumed to be close to zero (Laisk et al., 1989). Therefore, Eq. (7) simplifies to

$$F_{s,\text{O}_3} = -g_{s,\text{O}_3} \cdot c_{b,\text{O}_3} \quad (8)$$

If now surface reactions drastically reduce  $c_{b,\text{O}_3}$  (cf. Fig. 5b+d), the effective stomatal ozone flux  
 475 (see Supplement) and with that the effective ozone dose are also reduced, which eventually de-

termine the phytotoxic effects of ozone to plants (Massman, 2004). At this point, it is important to note that the uptake of non surface-reactive gases such as CO<sub>2</sub> is not affected by the altered ozone gradients.

Thus, whenever surface loss plays a role, both surface and stomatal ozone uptake by plants have to be considered together. Previous studies might therefore have overestimated stomatal ozone uptake (e.g. Kurpius and Goldstein, 2003; Cieslik, 2004; Goldstein et al., 2004; Fares et al., 2012). Hence, their reported stomatal ozone flux values should be considered as upper limits.

In future studies investigating the ozone depositions to vegetation, it might be worth to analyse also the surface composition of the plants. If the surfaces are covered with substantial amounts of unsaturated organic compounds, surface loss has to be considered right from the beginning in order not to overestimate stomatal ozone uptake. Due to the fact that surface reactions reduce ozone concentrations in the leaf boundary layer, it is not correct to calculate stomatal ozone loss applying the resistance scheme shown in Fig. 5a and to eventually define the surface loss of ozone as that portion of the total loss which is not explainable by gas phase reactions and stomatal uptake.

For real plants the altered ozone gradient profile shown in Fig. 5d is less pronounced depending on stomata depth, which reduces the total stomatal uptake, and reactive surface compounds, which show smaller surface reaction rates than assumed for the idealised 100% efficient ozone depleting surface (see Supplement). In the case of such a semi-reactive leaf surfaces a more sophisticated resistance scheme has to be used, which strongly complicates the calculation of stomatal and non-stomatal ozone fluxes (see Supplement and Fig. S4S5). Nonetheless, the simulations explain the experimentally observed behaviour of different tobacco plants very well.

### 3.8 Atmospheric implications

Over the last decade, several studies have shown discrepancies between measured and expected ozone deposition fluxes. Large downward ozone fluxes (Kurpius and Goldstein, 2003; Goldstein et al., 2004) (Kurpius and Goldstein, 2003; Goldstein et al., 2004; Fares et al., 2010) and high levels of oxidized VOC (Holzinger et al., 2005) have been taken as evidence for “unconventional in-canopy chemistry” of unknown precursors in a Ponderosa pine plantation, the Blodgett forest site. We speculate that to a certain extent these unknown precursors could be reactive compounds emitted or deposited onto the vegetation surfaces. Most recent results support this speculation. Measured ozone deposition fluxes could not be explained by modelled stomatal and known non-stomatal sinks, such as reactions with measured VOC in the gas phase (Wolfe et al., 2011a, b). The same observation was made by Rannik et al. (2012) in a Scots pine dominated field site in Hyytiälä. All these studies assume the presence of yet unmeasured highly reactive semi- or low-volatile compounds, which have a similar temperature dependent emission pattern as mono- and sesquiterpenes.

Wolfe et al. (2011b) assumed that the unmeasured reactive compounds might be unsaturated, cyclic terpenoids. Due to their low vapour pressure, the measurement of semi- or low volatile

compounds represents a challenge, since these substances strongly partition into the condensed phase and are therefore easily lost in the inlet systems of most current VOC instrumentation. However, Bouvier-Brown et al. (2007, 2009) were able to identify several different  
515 sesquiterpenes in ambient air and in branch enclosure experiments at the Blodgett forest site.

A large number of compounds with diterpenoid backbones were recently observed for the first time  
also in a in a different Ponderosa pine forest site during the BEACHON-RoMBAS campaign 2011  
(Chan et al., 2015). These unsaturated diterpenoids contain the same backbone as abietic acid, a  
primary component of resin acids. The observed temporal variations in concentrations were similar  
520 to those of sesquiterpenoids, suggesting they are directly emitted from the local vegetation.

Resins Most recently, Palm et al. (2015) have shown that semi- and intermediate volatility organic  
compounds measured for the first time at the same site with a novel thermal desorption electron  
impact mass spectrometer (TD-EIMS) could likely close the gap between observed and ex-  
pected secondary aerosol growth, estimated from gas-phase concentrations of the most abun-  
525 dant measured VOC (mono- and sesquiterpenes, toluene/p-cymene, isoprene). We therefore  
speculate that the high ozone deposition fluxes in such forest sites could be a result of not only  
gas-phase reactions, but to a certain extent also of ozone reactions with semi-volatiles emitted  
or redeposited onto the vegetation surfaces.

Possible sources of the measured and unmeasured higher terpenoids are – among others –  
530 constitutive plant emissions or resins, which are known to contain high amounts of sesqui-, di- and  
triterpenoids (Dell and McComb, 1979; Langenheim, 2003); di- and . Resins can be released during  
mechanical stress, e.g. in the event of hail storms (Bamberger et al., 2011) and could eventually  
evaporate depending on their vapour pressure (and therefore ambient temperature).

Di- and triterpenoids are also known constituents of surface waxes (Estell et al., 1994a, b; Altimir  
535 et al., 2008; Thimmappa et al., 2014). Moreover, it is estimated that about 30% of vascular plants  
have glandular trichomes, which often exude higher terpenoid compounds, too (Wagner et al., 2004).

All these terpenoid classes contain carbon-carbon double bonds and are therefore reactive with , and . Our results support the speculation that  
reaction rates of ozone with

Clearly, additional experiments are needed to better quantify the amount of semi-volatiles  
540 adsorbed at the surfaces are far higher than corresponding gas-phase ozonolysis rates. Thus, the fraction of volatile carbonyls produced in  
surface assisted ozonolysis of adsorbed semi-volatiles could compete with their respective gas-phase production rate from chemistry. To some  
extent this source of carbonyls in form of exudates or resins at the surface of particular plants might be obscured by the immediate uptake  
of the volatile ozonolysis products by the plants themselves (Karl et al., 2010; Niinemets et al., 2014). deposited onto vegetation  
surfaces and their impact on atmospheric chemistry.

545 Reactive surface compounds might also contribute to the varying ozone sensitivity of different conifer species (Schnitzler et al., 1999;  
Landolt et al., 2000) when exposed to the same cumulative ozone concentrations under light conditions. We anticipate therefore that surface  
ozonolysis plays an important role for the ozone tolerance of certain conifer species, too.

Our results also have relevance for other ozone-initiated processes that occur in the indoor and outdoor environment. Semi-volatile, unsaturated organic species are common on various surfaces including soil with plant litter (Weiss, 2000; Isidorov et al., 2003; Ormeño et al., 2009), aerosols (Rogge et al., 1993; D'Anna et al., 2009; Baduel et al., 2011), man-made structures (Wisthaler et al., 2005; Weschler et al., 2007; Shi and Zhao, 2015) and plant surfaces (Dell and McComb, 1979; Langenheim, 1994). These are therefore potential ozone sinks and sources of oxygenated VOC in ozone rich environments (see e.g. Wisthaler et al., 2005; Weschler et al., 2007; D'Anna et al., 2009; Baduel et al., 2011).

#### 4 Conclusions

Our results reveal for the first time a powerful ozone protection mechanism of plants having an ozone reactive leaf surface. This opportunistic defence mechanism, which is a beneficial side effect of semi-volatile terpenoids emitted onto the leaf surface, takes place before the phytotoxic gas enters the stomata. Plants emitting unsaturated semi-volatile compounds could have an advantageous effect for neighbouring plants as well: either directly by reducing overall ozone concentrations (see Supplement) or indirectly through the deposition of the semi-volatile compounds onto unprotected neighbouring leaves (Schmid et al., 1992; Himanen et al., 2010; Chan et al., 2015).

Reactive surface compounds might also contribute to the varying ozone sensitivity of different conifer species (Schnitzler et al., 1999; Landolt et al., 2000) when exposed to the same cumulative ozone concentrations under light conditions. We anticipate therefore that surface ozonolysis plays an important role for the ozone tolerance of certain conifer species, too.

Our findings have relevance not only for plants, but also for additional ozone-initiated processes that occur in the atmospheric boundary layer. The surface-assisted chemistry that we have elucidated for specific diterpenoids, linking for the first time volatile and non-volatile carbonyl products to semi-volatile precursors at the plant surface, is likely to occur also for other semi-volatile organic compounds on different surfaces, e.g. indoor and outdoor environment. Semi-volatile, unsaturated organic species are common on various surfaces including soil with plant litter (Weiss, 2000; Isidorov et al., 2003; Ormeño et al., 2009), aerosols (Rogge et al., 1993; D'Anna et al., 2009; Baduel et al., 2011), aerosols, man-made structures (Wisthaler et al., 2005; Weschler et al., 2007; Shi and Zhao, 2015) and even human skin (Wisthaler and Weschler, 2010). These are potential ozone sinks and sources of oxygenated VOC in ozone rich environments, as has been shown previously (Wisthaler and Weschler, 2010)(see e.g. Wisthaler et al., 2005; Weschler et al., 2007; D'Anna et al., 2009; Wisthaler and Weschler, 2010; Baduel et al., 2011). We speculate that some of the ozonolysis-derived products may play important roles in atmospheric processes, influencing the budgets of OH radicals and ozone. Conversely, in our experiments we had no indication that surface ozonolysis itself releases detectable amounts of OH radicals into the gas phase (see Supplement). In order to assess the global impact of surface-assisted ozonolysis on atmospheric chemistry a more complete knowledge about the nature of reactive, semi- and low-volatile compounds at plant surfaces as well as the mechanisms triggering their release (e.g. constitutive vs. biotic and mechanical stress induced emission) is needed.

## **Appendix A: Generation of the 3H02 variety – a *Nicotiana tabacum* line without diterpenoids**

The *Ambalema* variety which produces only *cis*-abienol and the *Colorado* variety which produces  
585 only CBTdiols (Sallaud et al., 2012) were crossed to produce hybrid F1 plants which produce both  
diterpenoids. Because the genetic loci responsible for the absence of CBTdiols and the absence of  
*cis*-abienol are distinct and unlinked, recombinant plants which produce neither diterpenoids could  
be recovered by analysing the leaf surface extracts by GC-MS in the selfed progeny of the F1 plants.  
One of these plants was selected, propagated over 2 generations by single seed descent and named  
590 line 3H02.

**The Supplement related to this article is available online at  
doi:10.5194/acp-0-1-2015-supplement.**

*Acknowledgements.* The authors would like to thank Francesco Loreto who initiated the tobacco experiments,  
Jörg-Peter (Jogi) Schnitzler for fruitful discussions and the gardeners of the Innsbruck University Botanic Gar-  
595 dens who grew the sample plants. W. Jud would like to thank Sheldon L. Cooper for helpful comments.

This project was financially supported by the European Science Foundation in the frame of the EuroVol  
MOMEVIP project and by the Austrian Fonds zur Förderung der wissenschaftlichen Forschung, project number  
I655-B16.

## References

- 600 Agathokleous, E., Saitanis, C. J., and Papatheohari, Y.: Evaluation of Di-1-p-Menthene as Antiozonant on Bel-W3 Tobacco Plants, as Compared with Ethylenediurea, *Water, Air, & Soil Pollution*, 225, 2139, doi:10.1007/s11270-014-2139-y, 2014.
- Altimir, N., Vesala, T., Aalto, T., Bäck, J., and Hari, P.: Stomatal-scale modelling of the competition between ozone sinks at the air-leaf interface, *Tellus, Series B: Chemical and Physical Meteorology*, 60 B, 381–391, doi:10.1111/j.1600-0889.2008.00344.x, 2008.
- 605 Ashmore, M. R.: Assessing the future global impacts of ozone on vegetation, *Plant Cell Environ.*, 28, 949–964, doi:10.1111/j.1365-3040.2005.01341.x, 2005.
- Atkinson, R. and Arey, J.: Atmospheric degradation of volatile organic compounds, *Chem. Rev.*, 103, 4605–4638, doi:10.1021/cr0206420, 2003.
- 610 Baduel, C., Monge, M. E., Voisin, D., Jaffrezo, J.-L., George, C., Haddad, I. E., Marchand, N., and D’Anna, B.: Oxidation of atmospheric humic like substances by ozone: a kinetic and structural analysis approach., *Environmental science & technology*, 45, 5238–44, doi:10.1021/es200587z, 2011.
- Ball, T.: Calculations related to gas exchange, in: *Stomatal Function*, edited by Zeiger, E., Farquhar, G. D., and Cowan, I. R., chap. 20, pp. 445–476, Stanford University Press, Stanford, 1987.
- 615 Bamberger, I., Hörtnagl, L., Ruuskanen, T. M., Schnitzhofer, R., Müller, M., Graus, M., Karl, T., Wohlfahrt, G., and Hansel, A.: Deposition fluxes of terpenes over grassland, *Journal of Geophysical Research*, 116, 1–13, doi:10.1029/2010JD015457, 2011.
- Borowiak, K., Zbierska, J., and Drapikowska, M.: Differences in morpho-anatomical structure of ozone-sensitive and ozone-resistant tobacco cultivars, *Acta Biologica Hungarica*, 61, 90–100, doi:10.1556/ABiol.61.2010.1.9, 2010.
- 620 Bouvier-Brown, N. C., Holzinger, R., Palitzsch, K., and Goldstein, A. H.: Quantifying sesquiterpene and oxygenated terpene emissions from live vegetation using solid-phase microextraction fibers, *Journal of Chromatography A*, 1161, 113–120, doi:10.1016/j.chroma.2007.05.094, 2007.
- Bouvier-Brown, N. C., Goldstein, A. H., Gilman, J. B., Kuster, W. C., and de Gouw, J. A.: In-situ ambient quantification of monoterpenes, sesquiterpenes, and related oxygenated compounds during BEARPEX 2007 – implications for gas- and particle-phase chemistry, *Atmospheric Chemistry and Physics*, 9, 5505–5518, doi:10.5194/acpd-9-10235-2009, 2009.
- 625 Breitenlechner, M. and Hansel, A.: Development of an Advanced Selective Reagent Ionization Time of Flight Mass Spectrometer (advanced SRI-TOF-MS), *Atmos. Meas. Tech. Discuss. Int. J. Mass Spectrom.*, submitted, 2015.
- 630 Caemmerer, S. and Farquhar, G. D.: Some relationships between the biochemistry of photosynthesis and the gas exchange of leaves, *Planta*, 153, 376–387, doi:10.1007/BF00384257, 1981.
- Cape, J. N., Hamilton, R., and Heal, M. R.: Reactive uptake of ozone at simulated leaf surfaces: implications for “non-stomatal” ozone flux, *Atmos. Environ.*, 43, 1116–1123, doi:10.1016/j.atmosenv.2008.11.007, 2009.
- 635 Chan, A. W. H., Kreisberg, N. M., Hohaus, T., Campuzano-Jost, P., Zhao, Y., Day, D. A., Kaser, L., Karl, T., Hansel, A., Teng, A. P., Ruehl, C. R., Sueper, D. T., Jayne, J. T., Worsnop, D. R., Jimenez, J. L., Hering, S. V., and Goldstein, A. H.: Speciated measurements of semivolatile and intermediate volatility organic

- compounds (S/IVOCs) in a pine forest during BEACHON-RoMBAS 2011, *Atmospheric Chemistry and Physics Discussions*, 15, 22 331–22 377, doi:10.5194/acpd-15-22331-2015, 2015.
- 640 Cieslik, S. A.: Ozone uptake by various surface types: a comparison between dose and exposure, *Atmos. Environ.*, 38, 2409–2420, doi:10.1016/j.atmosenv.2003.10.063, 2004.
- Criegee, R.: Mechanism of ozonolysis, *Angew. Chem. Int. Edit.*, 14, 745–752, 1975.
- D’Anna, B., Jammoul, A., George, C., Stemmler, K., Fahrni, S., Ammann, M., and Wisthaler, A.: Light-induced ozone depletion by humic acid films and submicron aerosol particles, *Journal of Geophysical Research*, 114, D12 301, doi:10.1029/2008JD011237, 2009.
- 645 Dell, B. and McComb, A. J.: Plant Resins-Their Formation, Secretion and Possible Functions, *Advances in Botanical Research*, 6, 277–316, doi:10.1016/S0065-2296(08)60332-8, 1979.
- Dentener, F., Stevenson, D., Ellingsen, K., Van Noije, T., Schultz, M., Amann, M., Atherton, C., Bell, N., Bergmann, D., Bey, I., Bouwman, L., Butler, T., Cofala, J., Collins, B., Drevet, J., Doherty, R., Eickhout, B., Eskes, H., Fiore, A., Gauss, M., Hauglustaine, D., Horowitz, L., Isaksen, I. S. A., Josse, B., Lawrence, M., Krol, M., Lamarque, J. F., Montanaro, V., Müller, J. F., Peuch, V. H., Pitari, G., Pyle, J., Rast, S., Rodriguez, J., Sanderson, M., Savage, N. H., Shindell, D., Strahan, S., Szopa, S., Sudo, K., Van Dingenen, R., Wild, O., and Zeng, G.: The global atmospheric environment for the next generation, *Environ. Sci. Technol.*, 40, 3586–3594, doi:10.1021/es0523845, 2006.
- 655 Eltayeb, A. E., Kawano, N., Badawi, G. H., Kaminaka, H., Sanekata, T., Shibahara, T., Inanaga, S., and Tanaka, K.: Overexpression of monodehydroascorbate reductase in transgenic tobacco confers enhanced tolerance to ozone, salt and polyethylene glycol stresses, *Planta*, 225, 1255–1264, doi:10.1007/s00425-006-0417-7, 2007.
- Enzell, C. R., Wahlberg, I., and Ryhage, R.: Mass spectra of tobacco isoprenoids, *Mass Spectrom. Rev.*, 3, 395–438, doi:10.1002/mas.1280030304, 1984.
- 660 Estell, R. E., Fredrickson, E. L., Anderson, D. M., Mueller, W. F., and Remmenga, M. D.: Relationship of Tarbush Leaf Surface Secondary Chemistry to Livestock Herbivory, *Journal of Range Management*, 47, 424–428, doi:10.2307/4002991, 1994a.
- Estell, R. E., Havstad, K. M., Fredrickson, E. L., and Gardea-Torresdey, J. L.: Secondary chemistry of the leaf surface of *Flourensia cernua*, *Biochemical Systematics and Ecology*, 22, 73–77, doi:10.1016/0305-1978(94)90116-3, 1994b.
- 665 Fahn, A.: Secretory tissues in vascular plants, *New Phytol.*, 108, 229–257, doi:10.1111/j.1469-8137.1988.tb04159.x, 1988.
- Fares, S., McKay, M., Holzinger, R., and Goldstein, A. H.: Ozone fluxes in a *Pinus ponderosa* ecosystem are dominated by non-stomatal processes: Evidence from long-term continuous measurements, *Agricultural and Forest Meteorology*, 150, 420–431, doi:10.1016/j.agrformet.2010.01.007, 2010.
- 670 Fares, S., Weber, R., Park, J.-H., Gentner, D., Karlik, J., and Goldstein, A. H.: Ozone deposition to an orange orchard: partitioning between stomatal and non-stomatal sinks, *Environ. Pollut.*, 169, 258–266, doi:10.1016/j.envpol.2012.01.030, 2012.
- 675 Felzer, B., Reilly, J., Melillo, J., Kicklighter, D., Sarofim, M., Wang, C., Prinn, R., and Zhuang, Q.: Future effects of ozone on carbon sequestration and climate change policy using a global biogeochemical model, *Climatic Change*, 73, 345–373, doi:10.1007/s10584-005-6776-4, 2005.

- Fruekilde, P., Hjorth, J., Jensen, N., Kotzias, D., and Larsen, B.: Ozonolysis at vegetation surfaces, *Atmos. Environ.*, 32, 1893–1902, doi:10.1016/S1352-2310(97)00485-8, 1998.
- 680 Fu, Y. and Tai, a. P. K.: Impact of climate and land cover changes on tropospheric ozone air quality and public health in East Asia between 1980 and 2010, *Atmospheric Chemistry and Physics*, 15, 10 093–10 106, doi:10.5194/acp-15-10093-2015, 2015.
- Gilbert, M. D., Elfving, D. C., and Lisk, D. J.: Protection of plants against ozone injury using the antiozonant N-(1,3-dimethylbutyl)-N'-phenyl-p-phenylenediamine, *Bulletin of Environmental Contamination and Toxicology*, 18, 783–786, doi:10.1007/BF01691993, 1977.
- 685 Goldstein, A. H., McKay, M., Kurpius, M. R., Schade, G. W., Lee, A., Holzinger, R., and Rasmussen, R. A.: Forest thinning experiment confirms ozone deposition to forest canopy is dominated by reaction with biogenic VOCs, *Geophys. Res. Lett.*, 31, L22106, doi:10.1029/2004GL021259, 2004.
- Goldstein, A. H. and Galbally, I. E.: Known and Unexplored Organic Constituents in the Earth's Atmosphere, *Environmental Science & Technology*, 41, 1514–1521, doi:10.1021/es072476p, 2007.
- 690 Granier, C., Bessagnet, B., Bond, T., D'Angiola, A., van der Gon, H. D., Frost, G. J., Heil, A., Kaiser, J. W., Kinne, S., Klimont, Z., Kloster, S., Lamarque, J. F., Liousse, C., Masui, T., Meleux, F., Mieville, A., Ohara, T., Raut, J. C., Riahi, K., Schultz, M. G., Smith, S. J., Thompson, A., van Aardenne, J., van der Werf, G. R., and van Vuuren, D. P.: Evolution of anthropogenic and biomass burning emissions of air pollutants at global and regional scales during the 1980-2010 period, *Climatic Change*, 109, 163–190, doi:10.1007/s10584-011-0154-1, 2011.
- Graus, M., Müller, M., and Hansel, A.: High resolution PTR-TOF: quantification and formula confirmation of VOC in real time, *J. Am. Soc. Mass Spectr.*, 21, 1037–1044, doi:10.1016/j.jasms.2010.02.006, 2010.
- Hansel, A., Singer, W., Wisthaler, A., Schwarzmann, M., and Lindinger, W.: Energy dependencies of the proton transfer reactions, *Int. J. Mass Spectrom.*, 167–168, 697–703, doi:10.1016/S0168-1176(97)00128-6, 1997.
- 700 Heggestad, H. E.: Origin of Bel-W3, Bel-C and Bel-B tobacco varieties and their use as indicators of ozone, *Environmental Pollution*, 74, 264–291, doi:10.1016/0269-7491(91)90076-9, 1991.
- Hewitt, C. N., Kok, G. L., and Fall, R.: Hydroperoxides in plants exposed to ozone mediate air pollution damage to alkene emitters, *Nature*, 344, 56–58, doi:10.1038/344056a0, 1990.
- 705 Himanen, S. J., Blande, J. D., Klemola, T., Pulkkinen, J., Heijari, J., and Holopainen, J. K.: Birch (*Betula* spp.) leaves adsorb and re-release volatiles specific to neighbouring plants - a mechanism for associational herbivore resistance?, *New Phytologist*, 186, 722–732, doi:10.1111/j.1469-8137.2010.03220.x, 2010.
- Holzinger, R., Lee, A., Paw, K. T., and Goldstein, U. A. H.: Observations of oxidation products above a forest imply biogenic emissions of very reactive compounds, *Atmos. Chem. Phys.*, 5, 67–75, doi:10.5194/acp-5-67-2005, 2005.
- 710 IPCC: *Climate Change 2013: The Physical Science Basis. Contribution of Working Group I to the Fifth Assessment Report of the Intergovernmental Panel on Climate Change*, Cambridge University Press, Cambridge, United Kingdom and New York, NY, USA, 2013.
- Isidorov, V. A., Vinogorova, V. T., and Rafałowski, K.: HS-SPME analysis of volatile organic compounds of coniferous needle litter, *Atmospheric Environment*, 37, 4645–4650, doi:10.1016/j.atmosenv.2003.07.005, 2003.



- Jenkin, M. E. and Clemitshaw, K. C.: Ozone and other secondary photochemical pollutants: chemical processes governing their formation in the planetary boundary layer, *Atmos. Environ.*, 34, 2499–2527, doi:10.1016/S1352-2310(99)00478-1, 2000.
- 720 Karl, T., Harley, P., Emmons, L., Thornton, B., Guenther, A., Basu, C., Turnipseed, A. and Jardine, K.: Efficient atmospheric cleansing of oxidized organic trace gases by vegetation, *Science*, 330, 816–819, doi:10.1126/science.1192534, 2010.
- Karl, T., Hansel, A., Cappellin, L., Kaser, L., Herdinger-Blatt, I., and Jud, W.: Selective measurements of isoprene and 2-methyl-3-buten-2-ol based on  $\text{NO}^+$  ionization mass spectrometry, *Atmos. Chem. Phys.*, 12, 11877–11884, doi:10.5194/acp-12-11877-2012, 2012.
- 725 Kennedy, B. S., Nielsen, M. T., Severson, R. F., Sisson, V. A., Stephenson, M. K., and Jackson, D. M.: Leaf surface chemicals from *Nicotiana* affecting germination of *Peronospora tabacina* (adam) sporangia, *J. Chem. Ecol.*, 18, 1467–1479, doi:10.1007/BF00993221, 1992.
- Kennedy, B. S., Nielsen, M. T., and Severson, R. F.: Biorationals from *Nicotiana* protect cucumbers against *Colletotrichum lagenarium* (Pass.) ell. & halst disease development, *J. Chem. Ecol.*, 21, 221–231, doi:10.1007/BF02036653, 1995.
- 730 Kurpius, M. R. and Goldstein, A. H.: Gas-phase chemistry dominates  $\text{O}_3$  loss to a forest, implying a source of aerosols and hydroxyl radicals to the atmosphere, *Geophys. Res. Lett.*, 30, 1371, doi:10.1029/2002GL016785, 2003.
- 735 Laisk, A., Kull, O., and Moldau, H.: Ozone concentration in leaf intercellular air spaces is close to zero, *Plant Physiol.*, 90, 1163–1167, 1989.
- Landolt, W., Bühlmann, U., Bleuler, P., and Bucher, J. B.: Ozone exposure–response relationships for biomass and root/shoot ratio of beech (*Fagus sylvatica*), ash (*Fraxinus excelsior*), Norway spruce (*Picea abies*) and Scots pine (*Pinus sylvestris*), *Environ. Pollut.*, 109, 473–478, doi:10.1016/S0269-7491(00)00050-6, 2000.
- 740 Langenheim, J. H.: Higher plant terpenoids: A phytocentric overview of their ecological roles, *Journal of Chemical Ecology*, 20, 1223–1280, doi:10.1007/BF02059809, 1994.
- Langenheim, J. H.: *Plant Resins: Chemistry, Evolution, Ecology, and Ethnobotany*, Timber Press, Portland, Cambridge, 2003.
- Lin, Y. and Wagner, G. J.: Surface disposition and stability of pest-interactive, trichome-exuded diterpenes and sucrose esters of tobacco, *J. Chem. Ecol.*, 20, 1907–1921, doi:10.1007/BF02066232, 1994.
- 745 Logan, J. a., Stachelin, J., Megretskaia, I. A., Cammas, J. P., Thouret, V., Claude, H., De Backer, H., Steinbacher, M., Scheel, H. E., Stbi, R., Frhlich, M., and Derwent, R.: Changes in ozone over Europe: Analysis of ozone measurements from sondes, regular aircraft (MOZAIC) and alpine surface sites, *Journal of Geophysical Research: Atmospheres*, 117, 1–23, doi:10.1029/2011JD016952, 2012.
- 750 Loreto, F., Mannozi, M., Maris, C., Nascetti, P., Ferranti, F., and Pasqualini, S.: Ozone quenching properties of isoprene and its antioxidant role in leaves., *Plant Physiology*, 126, 993–1000, doi:10.1104/pp.126.3.993, 2001.
- Loreto, F. and Fares, S.: Is ozone flux inside leaves only a damage indicator? Clues from volatile isoprenoid studies, *Plant Physiol.*, 143, 1096–1100, doi:10.1104/pp.106.091892, 2007.

- 755 Massman, W. J.: Toward an ozone standard to protect vegetation based on effective dose: a review of deposition resistances and a possible metric, *Atmos. Environ.*, 38, 2323–2337, doi:10.1016/j.atmosenv.2003.09.079, 2004.
- Moldau, H. and Bichele, I.: Plasmalemma protection by the apoplast as assessed from above-zero ozone concentrations in leaf intercellular air spaces, *Planta*, 214, 484–487, doi:10.1007/s00425-001-0678-0, 2002.
- 760 Monson, R. and Baldocchi, D.: *Terrestrial Biosphere-Atmosphere Fluxes*, Cambridge University Press, New York, 2014.
- Müller, M., Mikoviny, T., Jud, W., D’Anna, B., and Wisthaler, A.: A new software tool for the analysis of high resolution PTR-TOF mass spectra, *Chemometr. Intell. Lab.*, 127, 158–165, doi:10.1016/j.chemolab.2013.06.011, 2013.
- 765 Neubert, A., Kley, D., Wildt, J., Segschneider, H., and Förstel, H.: Uptake of NO, NO<sub>2</sub> and O<sub>3</sub> by sunflower (*Helianthus annuus* L.) and tobacco plants (*Nicotiana tabacum* L.): dependence on stomatal conductivity, *Atmos. Environ. A-Gen.*, 27, 2137–2145, doi:10.1016/0960-1686(93)90043-X, 1993.
- Niinimets, Ü., Fares, S., Harley, P., and Jardine, K. J.: Bidirectional exchange of biogenic volatiles with vegetation: Emission sources, reactions, breakdown and deposition, *Plant Cell Environ.*, 37, 1790–1809, doi:10.1111/pce.12322, 2014.
- 770 Oltmans, S., Lefohn, A., Shadwick, D., Harris, J., Scheel, H., Galbally, I., Tarasick, D., Johnson, B., Brunke, E.-G., Claude, H., Zeng, G., Nichol, S., Schmidlin, F., Davies, J., Cuevas, E., Redondas, A., Naoe, H., Nakano, T., and Kawasato, T.: Recent tropospheric ozone changes – A pattern dominated by slow or no growth, *Atmospheric Environment*, 67, 331–351, doi:10.1016/j.atmosenv.2012.10.057, 2013.
- 775 Ormeño, E., Céspedes, B., Sánchez, I. A., Velasco-García, A., Moreno, J. M., Fernandez, C., and Baldy, V.: The relationship between terpenes and flammability of leaf litter, *Forest Ecology and Management*, 257, 471–482, doi:10.1016/j.foreco.2008.09.019, 2009.
- Palm, B. B., Campuzano-Jost, P., Ortega, A. M., Day, D. A., Karl, T., Kaser, L., Jud, W., Hansel, A., Hunter, J. F., Kroll, J. H., Brune, W. H., and Jimenez, J. L.: In-situ Secondary Organic Aerosol Formation in ambient pine forest air using an oxidation flow reactor, *Atmospheric Chemistry and Physics Discussions* 15, 30409–30471, doi:10.5194/acpd-15-30409-2015, 2015.
- 780 Palmer-Young, E. C., Veit, D., Gershenson, J., and Schuman, M. C.: The Sesquiterpenes (E)- $\beta$ -Farnesene and (E)- $\alpha$ -Bergamotene Quench Ozone but Fail to Protect the Wild Tobacco *Nicotiana attenuata* from Ozone, UVB, and Drought Stresses, *Plos One*, pp. 1–22, doi:10.5061/dryad.602d6, 2015.
- 785 Parrish, D. D., Law, K. S., Staehelin, J., Derwent, R., Cooper, O. R., Tanimoto, H., Volz-Thomas, A., Gilge, S., Scheel, H. E., Steinbacher, M., and Chan, E.: Long-term changes in lower tropospheric baseline ozone concentrations at northern mid-latitudes, *Atmospheric Chemistry and Physics*, 12, 11485–11504, doi:10.5194/acp-12-11485-2012, 2012.
- Rannik, Ü., Altimir, N., Mammarella, I., Bäck, J., Rinne, J., Ruuskanen, T. M., Hari, P., Vesala, T., and Kulmala, M.: Ozone deposition into a boreal forest over a decade of observations: evaluating deposition partitioning and driving variables, *Atmospheric Chemistry and Physics*, 12, 12165–12182, doi:10.5194/acp-12-12165-2012, 2012.
- 790

- Rogge, W. F., Hildemann, L. M., Mazurek, M. A., Cass, G. R., and Simoneit, B. R. T.: Sources of fine organic aerosol. 4. Particulate abrasion products from leaf surfaces of urban plants, *Environ. Sci. Technol.*, 27, 2700–2711, doi:10.1021/es00049a008, 1993.
- 795 Sallaud, C., Giacalone, C., Töpfer, R., Goepfert, S., Bakaher, N., Rösti, S., and Tissier, A.: Characterization of two genes for the biosynthesis of the labdane diterpene Z-abienol in tobacco (*Nicotiana tabacum*) glandular trichomes, *Plant J.*, 72, 1–17, doi:10.1111/j.1365-313X.2012.05068.x, 2012.
- Schmid, C., Steinbrecher, R., and Ziegler, H.: Partition coefficients of plant cuticles for monoterpenes, *Trees*, 6, 32–36, doi:10.1007/BF00224496, 1992.
- 800 Schnitzler, J. P., Langebartels, C., Heller, W., Liu, J., Lippert, M., Dohring, T., Bahnweg, G., and Sander-  
mann, H.: Ameliorating effect of UV-B radiation on the response of Norway spruce and Scots pine to ambient  
ozone concentrations, *Glob. Change Biol.*, 5, 83–94, doi:10.1046/j.1365-2486.1998.00208.x, 1999.
- Schraudner, M., Moeder, W., Wiese, C., Van Camp, W., Inzé, D., Langebartels, C., and Sandermann, H.:  
805 Ozone-induced oxidative burst in the ozone biomonitor plant, tobacco Bel W3, *Plant Journal*, 16, 235–245,  
doi:10.1046/j.1365-313X.1998.00294.x, 1998.
- Shi, S. and Zhao, B.: Estimating indoor semi-volatile organic compounds (SVOCs) associated with settled dust  
by an integrated kinetic model accounting for aerosol dynamics, *Atmospheric Environment*, 107, 52–61,  
doi:10.1016/j.atmosenv.2015.01.076, 2015.
- 810 Singh, S. and Agrawal, S. B.: Impact of tropospheric ozone on wheat (*Triticum aestivum* L.) in the eastern  
Gangetic plains of India as assessed by ethylenediurea (EDU) application during different developmental  
stages, *Agriculture, Ecosystems and Environment*, 138, 214–221, doi:10.1016/j.agee.2010.04.020, 2010.
- Sitch, S., Cox, P. M., Collins, W. J., and Huntingford, C.: Indirect radiative forcing of climate change through  
ozone effects on the land-carbon sink, *Nature*, 448, 791–794, doi:10.1038/nature06059, 2007.
- 815 Španěl, P., Ji, Y., and Smith, D.: SIFT studies of the reactions of  $\text{H}_3\text{O}^+$ ,  $\text{NO}^+$  and  $\text{O}_2^+$  with a series of aldehydes  
and ketones, *Int. J. Mass Spectrom.*, 165–166, 25–37, doi:10.1016/S0168-1176(97)00166-3, 1997.
- Thimmappa, R., Geisler, K., Louveau, T., O'Maille, P., and Osbourn, A.: Triterpene biosynthesis in plants,  
*Annu. Rev. Plant Biol.*, 65, 225–257, doi:10.1146/annurev-arplant-050312-120229, 2014.
- Van Dingenen, R., Dentener, F. J., Raes, F., Krol, M. C., Emberson, L., and Cofala, J.: The global impact  
820 of ozone on agricultural crop yields under current and future air quality legislation, *Atmos. Environ.*, 43,  
604–618, doi:10.1016/j.atmosenv.2008.10.033, 2009.
- Vickers, C. E., Gershenzon, J., Lerdau, M. T., and Loreto, F.: A unified mechanism of action for volatile iso-  
prenoids in plant abiotic stress., *Nature Chemical Biology*, 5, 283–291, doi:10.1038/nchembio.158, 2009a.
- Vickers, C. E., Possell, M., Cojocariu, C. I., Velikova, V. B., Laothawornkitkul, J., Ryan, A., Mullineaux, P. M.,  
825 and Hewitt, C. N.: Isoprene synthesis protects transgenic tobacco plants from oxidative stress., *Plant, Cell  
and Environment*, 32, 520–531, doi:10.1111/j.1365-3040.2009.01946.x, 2009b.
- Vingarzan, R.: A review of surface ozone background levels and trends, *Atmos. Environ.*, 38, 3431–3442,  
doi:10.1016/j.atmosenv.2004.03.030, 2004.
- Wagner, G. J.: Secreting glandular trichomes: more than just hairs, *Plant Physiol.*, 96, 675–679, 1991.
- 830 Wagner, G. J., Wang, E. and Shepherd, R. W.: New Approaches for Studying and Exploiting an Old Protuber-  
ance, the Plant Trichome, *Annals of Botany*, 93, 3–11, doi:10.1093/aob/mch011, 2004.

- Wang, X. and Mauzerall, D. L.: Characterizing distributions of surface ozone and its impact on grain production in China, Japan and South Korea: 1990 and 2020, *Atmos. Environ.*, 38, 4383–4402, doi:10.1016/j.atmosenv.2004.03.067, 2004.
- 835 Weiss, P.: Vegetation/Soil Distribution of Semivolatile Organic Compounds in Relation to Their Physicochemical Properties, *Environmental Science & Technology*, 34, 1707–1714, doi:10.1021/es990576s, 2000.
- Weschler, C. J., Wisthaler, A., Cowlin, S., Tamás, G., Strøm Tejsen, P., Hodgson, A. T., Destailats, H., Herrington, J., Zhang, J., and Nazaroff, W. W.: Ozone-initiated chemistry in an occupied simulated aircraft cabin, *Environmental Science and Technology*, 41, 6177–6184, doi:10.1021/es0708520, 2007.
- 840 Wisthaler, A., Tamás, G., Wyon, D. P., Strøm Tejsen, P., Space, D., Beauchamp, J., Hansel, A., Märk, T. D., and Weschler, C. J.: Products of ozone-initiated chemistry in a simulated aircraft environment, *Environmental Science and Technology*, 39, 4823–4832, doi:10.1021/es047992j, 2005.
- Wisthaler, A. and Weschler, C. J.: Reactions of ozone with human skin lipids: sources of carbonyls, dicarbonyls, and hydroxycarbonyls in indoor air, *P. Natl. Acad. Sci. USA*, 107, 6568–6575, doi:10.1073/pnas.0904498106, 2010.
- 845 Wohlfahrt, G., Hörtnagl, L., Hammerle, A., Graus, M., and Hansel, A.: Measuring eddy covariance fluxes of ozone with a slow-response analyser, *Atmospheric Environment*, 43, 4570–4576, doi:10.1016/j.atmosenv.2009.06.031, 2009.
- Wohlgenuth, H., Mittelstrass, K., Kschieschan, S., Bender, J., Weigel, H.-J., Overmyer, K., Kangasjarvi, J., Sandermann, H., and Langebartels, C.: Activation of an oxidative burst is a general feature of sensitive plants exposed to the air pollutant ozone, *Plant Cell Environ.*, 25, 717–726, doi:10.1046/j.1365-3040.2002.00859.x, 2002.
- 855 Wolfe, G. M., Thornton, J. A., Bouvier-Brown, N. C., Goldstein, A. H., Park, J.-H., McKay, M., Matross, D. M., Mao, J., Brune, W. H., LaFranchi, B. W., Browne, E. C., Min, K.-E., Wooldridge, P. J., Cohen, R. C., Crouse, J. D., Faloona, I. C., Gilman, J. B., Kuster, W. C., de Gouw, J. A., Huisman, A., and Keutsch, F. N.: The Chemistry of Atmosphere-Forest Exchange (CAFE) Model – Part 2: Application to BEARPEX-2007 observations, *Atmospheric Chemistry and Physics*, 11, 1269–1294, doi:10.5194/acp-11-1269-2011, 2011.
- 860 Wolfe, G. M., Thornton, J. A., McKay, M., and Goldstein, A. H.: Forest-atmosphere exchange of ozone: Sensitivity to very reactive biogenic VOC emissions and implications for in-canopy photochemistry, *Atmospheric Chemistry and Physics*, 11, 7875–7891, doi:10.5194/acp-11-7875-2011, 2011.

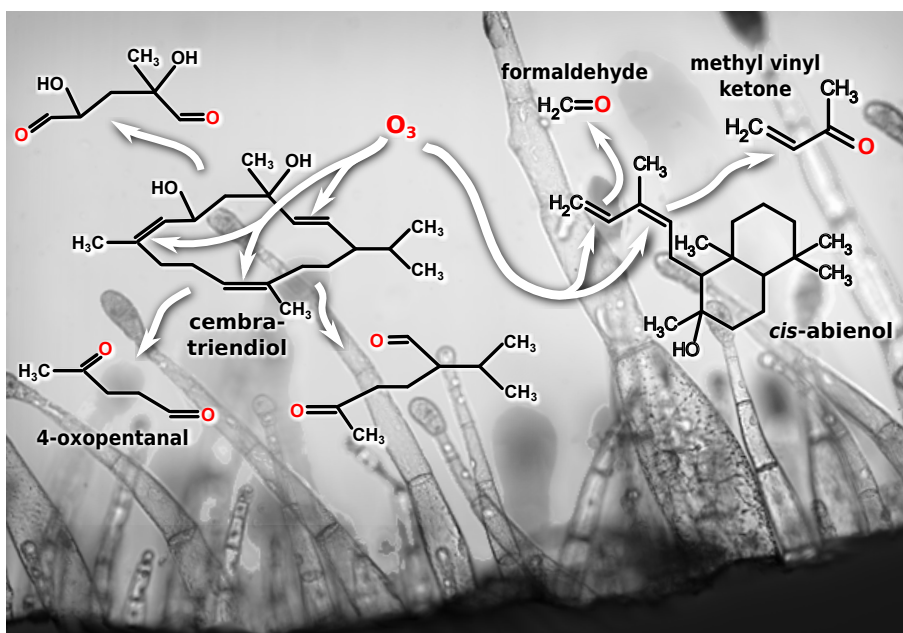


**Figure 1.** Ozonolysis of diterpenoids exuded by the trichomes of the investigated tobacco plants. The *BYBA* variety releases  $\alpha$ - and  $\beta$ -cembratrien-diols ( $C_{20}H_{34}O_2$ ), the *Ambalema* variety *cis*-abienol ( $C_{20}H_{34}O$ ); the *Basma Drama* variety exudes all these compounds. Ozonolysis of the cembratriendiols requires at least two ozonolysis steps to form short-chained, volatile carbonyls, like e.g. 4-oxopentanal ( $C_5H_8O_2$ ). Ozonolysis of *cis*-abienol leads to the formation of volatile formaldehyde ( $HCHO$ ) and methyl vinyl ketone ( $C_4H_6O$ ). The background image shows glandular trichomes on a tobacco leaf.

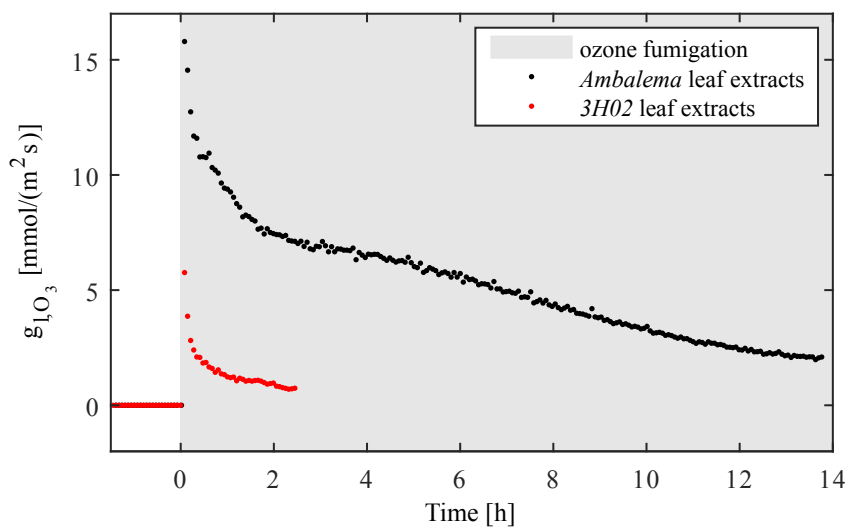


**Figure 2.** Ozonolysis experiments with pure leaf exudates extracted from non ozone fumigated, unimpaired plants. The leaf extracts containing the surface compounds were applied to the inner surface of the empty plant enclosure system (see Materials and methods section). During ozone fumigation (grey shaded area), the total ozone conductance  $g_{l,O_3}$  to the enclosure surface was much higher for *Ambalema* leaf extracts (containing large amounts of the diterpenoid *cis*-abienol) than for 3H02 extracts. Moreover, it remained high for many hours.

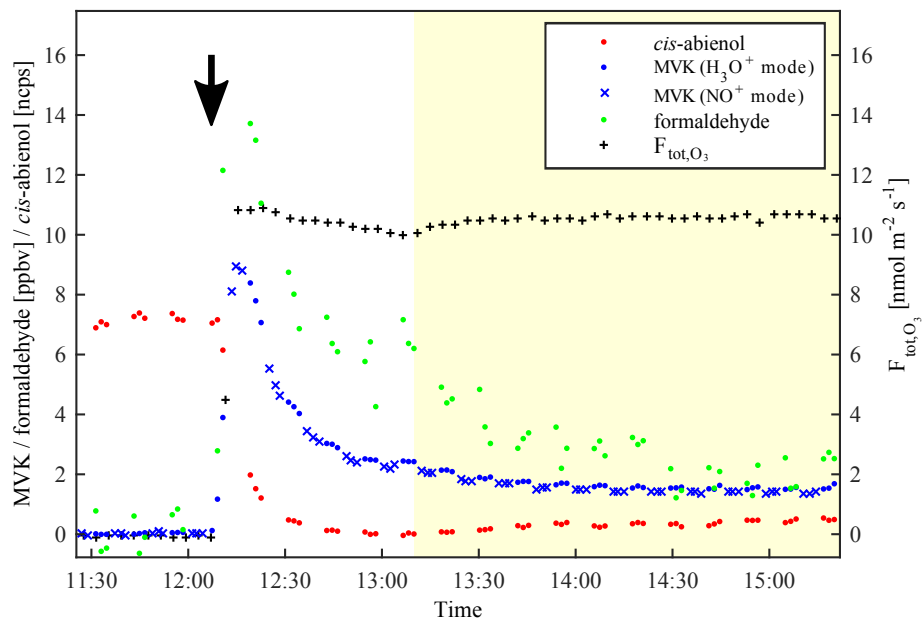


**Figure 3.** Temporal evolution of selected VOC in an ozonolysis experiment with an *Ambalema* plant and corresponding total ozone deposition flux  $F_{\text{tot},\text{O}_3}$ . The yellow shaded area denotes time ranges, in which the sample plant was illuminated. Starting the fumigation with  $\sim 60$  ppbv ozone (indicated by the black arrow) the *cis*-abienol signal decreased quickly. At the same time, the carbonyl products of *cis*-abienol ozonolysis, formaldehyde and MVK (measured in  $\text{H}_3\text{O}^+$  respectively  $\text{NO}^+$  reagent ion mode of the SRI-ToF-MS), started to rise. The large scattering of the formaldehyde signal derives from the strongly reduced sensitivity of the SRI-ToF-MS under high humidity conditions towards this compound. Two hours after the start of the ozone fumigation an equilibrium between actual diterpenoid production and loss due to surface reactions was established, resulting in stable signals of the oxygenated VOC.

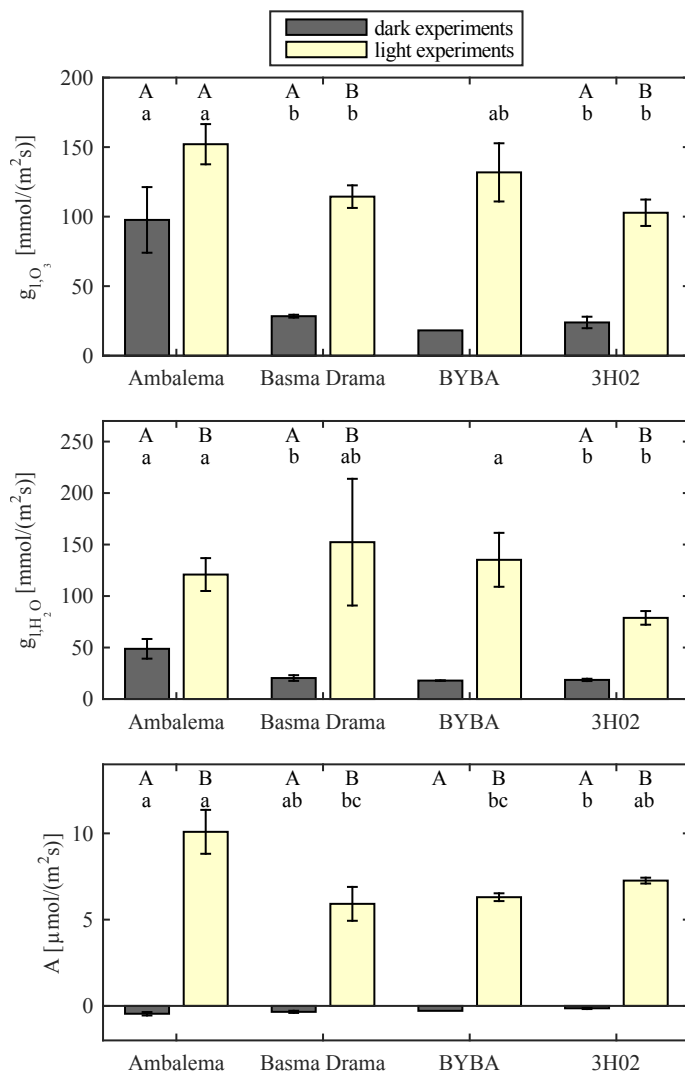


**Figure 4.** Total ozone conductance  $g_{1,O_3}$  (a), total water vapour conductance  $g_{1,H_2O}$  (b) and assimilation rates  $A$  (c) of different tobacco varieties during dark and light conditions. Error bars denote the standard error of 5 (13), 2 (6), 1 (5) and 3 (5) replicates of *Ambalema*, *Basma Drama*, *BYBA* respectively 3H02 in dark (light) experiments. Different capital letters denote significant different means in light and dark experiments of the same plant type and lower case letters significant different means of different plant types in either dark or light experiments, respectively (Wilcoxon-Mann-Whitney test,  $p < 0.1$ , see Methods part. Lacking replicates, in the statistical analysis dark experiments using *BYBA* plants were omitted). Under dark conditions stomatal ozone conductance is generally low and consequently surface reactions are the major ozone sink. The surface sink is high for the *Ambalema* tobacco line, which exudes *cis*-abienol and lower for the other lines, exuding less reactive or no diterpenoids.



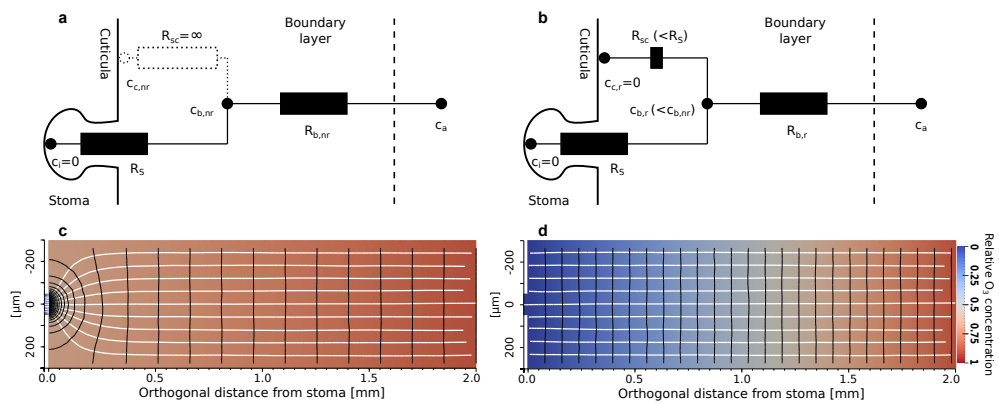


**Figure 5.** Fluid dynamic calculations of ozone uptake by stomata and leaf surface. **(a and b)** show the resistance schemes for ozone uptake of leaves with non-reactive (nr) and reactive (r) surfaces.  $c_i$ ,  $c_c$ ,  $c_b$  and  $c_a$  denote ozone concentrations in the stomatal cavity, at the leaf surface, in the boundary layer and in ambient air, respectively.  $R_s$  and  $R_b$  denote the stomatal and boundary layer resistances. The surface chemical resistance  $R_{sc}$  is infinite ( $R_{sc} = \infty$ ) on a non-reactive surface. Fluid dynamic calculations reveal ozone concentration gradients (white lines indicate their orientation) evolving parallel and perpendicular to the leaf surface around the stoma (located at the coordinate (0,0)) in this case **(c)**. If the leaf surface is covered with ozone-reactive substances, the parallel fraction of the ozone gradients vanishes, resulting in isosurfaces of ozone concentration (black lines) parallel to the leaf surface and stronger ozone depletion in the leaf boundary layer **(d)**.

# 1 The fate of the Criegee Intermediates

In our experiments we focused mainly on stable and volatile ozonolysis products, since these are the only ones directly accessible with SRI-ToF-MS. However, according to current understanding, there are many more possible ozonolysis products. Some of them are very short-lived, others too little volatile and therefore not measurable in the gas phase.

The Criegee mechanism (Criegee, 1975) predicts for gas phase ozone - alkene reactions a decomposition of the primary ozone-alkene addition product into a primary carbonyl compound and a highly excited Criegee Intermediate (CI). On the one hand, unimolecular reactions of unsubstituted (or monosubstituted) anti-CI conformers (terminal oxygen atom faces a hydrogen atom) are believed to yield excited organic acids, which might further dissociate to OH, H and organic radicals (Kroll et al., 2001). On the other hand, unimolecular reactions of disubstituted (or monosubstituted) syn-carbonyl oxides (terminal oxygen faces an alkyl group) are thought to form vinyl hydroperoxide intermediates (Kroll et al., 2001; Cremer, 1981), which will eventually decay forming OH radicals, too. In any case, the OH radicals formed in homogeneous ozone - alkene reactions play an important role in atmospheric chemistry, since their reaction rates with VOC are generally much higher than those of ozone (Atkinson and Arey, 2003). Atmospheric oxidation of VOC in regions with high NO<sub>x</sub> concentrations leads again to the formation of ozone (Jenkin and Clemitshaw, 2000). The OH radical recycling is therefore crucial for the oxidizing capacity of the atmosphere.

However, in surface ozonolysis it can be assumed that the energy rich CI is efficiently relaxed through collisions at the surface, thus forming a Stabilized Criegee Intermediate (SCI). If this is the case, we would expect no OH formation from CI in the gas phase. In order to prove this hypothesis we've added cyclohexane as OH scavenger in some of our tobacco experiments. The results indeed indicate that no OH is released into or formed in the gas phase. Nonetheless, we cannot totally exclude OH formation from ozonolysis at the plant surface, where these radicals would be readily scavenged by reactive compounds (e.g. diterpenoids).

In the condensed phase additional reaction pathways for the SCI become available. First, it could undergo a 1,3-cycloaddition with the corresponding ozonolysis carbonyl in order to form a secondary ozonide (Criegee, 1975; Finlayson-Pitts and Pitts, 2000).

Secondly, different isomerisation reactions of the CI could result in stable products. The so-called hot organic acid from anti-CI might be collisionally stabilized at the surface. In the *cis*-abienol case one would expect formic acid from the CI formed in the ozonolysis of the terminal double bond. Formic acid is volatile enough and was detected by SRI-ToF-MS.

In the condensed phase the syn-CI could form a vinyl hydroperoxide which might isomerise to stable  $\alpha$ -hydroxy ketones (Epstein and Donahue, 2008). Such molecules were found in ozonolysis experiments of skin oils containing squalene as major constituent (Wisthaler and Weschler, 2010). Indeed, we were able

to detect a compound at  $m/z$ 87.045 ( $C_4H_7O_2^+$ ) and  $m/z$ 116.035 ( $C_4H_6O_2 \bullet NO^+$ ) in  $H_3O^+$  respectively  $NO^+$  reagent ion mode, tentatively assigned to  $\alpha$ -hydroxy-2-butenone. This compound could be formed along with MVK when the inner double bond of *cis*-abienol (see Fig. 1a) is attacked by ozone.

In the humid plant chamber environment (relative humidity ranged from about 55 % during dark conditions to > 80 % when plants were illuminated) reactions of the SCI in the liquid water layer at the plant surface could also form hydroxy-alkyl hydroperoxides. These could again decay forming carbonyls, acids, hydrogen peroxides, water and OH radicals, as known from gas phase reactions (Hasson et al., 2003).

## 2 Non-volatile ozonolysis carbonyls

As mentioned in the previous section, fragmentation of the ozone-alkene addition complex yields a carbonyl and a CI. In the case of *cis*-abienol ozonolysis, along with the volatile carbonyls MVK and formaldehyde also the corresponding longer chained carbonyls should be formed. These  $C_{16}$  respectively  $C_{19}$  compounds are expected to be non-volatile due to their estimated vapour pressure (Goldstein and Galbally, 2007) and will thus remain at the leaf surface. In order to test this, we stripped off the leaf surface compounds after the ozone fumigation experiments as described in the Materials and methods part. The samples were then analysed by GC-MS (see Materials and methods). However, lacking reference spectra of most of the expected non-volatile ozonolysis products, peak assignment was difficult. Nonetheless we could assign a peak with high certainty to sclaral, an isomerisation product of the  $C_{16}$  carbonyl from *cis*-abienol ozonolysis. Moreover we were able to detect large amounts of unreacted *cis*-abienol and CBTdiols in samples of the corresponding emitter plant.

## 3 Surface ozonolysis in tubing and at the plant enclosure surface

The diterpenoids released by the tobacco plants are semi- or low volatile. These terms usually refer to compounds having a low vapour pressure and high boiling point at room temperature (Goldstein and Galbally, 2007). Consequently, under standard conditions they remain mainly in the liquid or solid phase. This is for example the case for the diterpenoid *cis*-abienol, which is a solid at room temperature. Nonetheless, to some extent semi-volatile diterpenoids can evaporate into the gas phase and be deposited in places remote from their point of emission. Continuous condensation and evaporation of the semi-volatile compounds leads to an equilibrium between the gas and condensed phase.

In our experiments plants were installed in the plant enclosure the day before the actual measurement, so that they could adapt and recover from any stress experienced in the course of installation. During plant acclimation the plant enclosure was continuously flushed with clean, ozone free air. Since for example the semi-volatile *cis*-abienol (exuded by the *Ambalema* or *Basma Drama* trichomes) slowly evaporated into the gas phase, it covered over time - when ozone was not present - not only the plant surface, but

also the inner surface of the plant enclosure and the downstream tubing system. As a consequence, the *cis*-abienol covered surface area was increased. In the presence of ozone, the adsorbed *cis*-abienol at the enclosure and tubing surfaces was quickly depleted. This effect was responsible for bursts of the volatile diterpenoid oxidation products at the beginning of ozone fumigation (cf. Fig. 3). Eventually, a new equilibrium between diterpenoid production by the plant’s trichomes and diterpenoid loss due to surface ozonolysis was established, along with a stable, positive carbonyl signal. Freshly deposited *cis*-abienol was then prevalingly covering the plant surface, which is closest to the trichomes.

To further investigate the impact of the surface ozonolysis in the tubing and at the enclosure surface, additional experiments with two plant enclosures in a row were conducted. To this end, the incoming air stream (see Materials and methods section) was split up in two parts. About  $\sim 90\%$  of the flow was directed into the first plant enclosure containing a sample plant. The residual part ( $\sim 10\%$ ) was directed through an ozone generator and could thereby be enriched with ozone. The air containing ozone could then be added either to the first plant enclosure or to the second, empty chamber. Fig. S1 shows the resulting MVK signal from *cis*-abienol ozonolysis in an experiment with an *Ambalema* plant. Ozone addition to the empty plant enclosure caused a short and less intense MVK burst deriving from surface ozonolysis of *cis*-abienol deposited during plant acclimation at the surface of the second chamber and tubing. After about 30 min ( $\sim 3$  gas exchange times of the chamber) the MVK signal became insignificant indicating that the surface deposited *cis*-abienol was consumed by ozonolysis and very few *cis*-abienol was resupplied by the air flow originating from the enclosure containing the sample plant. This implicates that gas phase reactions between *cis*-abienol and ozone are not relevant under fast gas exchange rates. When in a second step the flow of ozonized air was directed to the first enclosure containing the sample plant, again a large burst of MVK from *cis*-abienol ozonolysis on all surfaces was observed. However, in contrast to the previous experiment, after a certain time span the MVK signal approximated a plateau well above the background level.

## 4 Relative humidity during ozone fumigation experiments

Several studies have reported on a humidity dependent ozone uptake of different plant types (see e.g. Lamaud et al., 2002; Altimir et al., 2004, 2006). Non-stomatal ozone deposition has been shown to increase significantly above a relative humidity (RH) of about 70% (Lamaud et al., 2002; Altimir et al., 2006).

In our experiments the *Ambalema* variety showed a high total ozone conductance under dark conditions, which was about 4 – 5 times higher than that of all other varieties. This cannot be explained by the RH alone. The relative humidities measured at the enclosure outlet were well below 70% in all dark experiments, ranging from  $\sim 54\%$  –  $\sim 62\%$  (see Table S1). We conclude therefore that the RH had only

a minor impact on the total ozone conductance of the varieties tested.

## 5 2-day simulations of ozone protection through surface diterpenoids

In order to test the long term ozone protection efficiency of a leaf surface covered with diterpenoids, we conducted experiments lasting for two days (see Fig. S2). In the course of these experiments the ozone concentration in the plant enclosure was altered from 0-60 ppbv, mimicking diurnal ozone variations in the atmosphere. In experiments using *cis*-abienol emitters, the start of ozone fumigation led to the well-known rise of the corresponding oxidation products formaldehyde and MVK. Under light conditions and 20 ppbv ozone the *cis*-abienol signal dropped close to the detection limit. However, during the simulated night and without O<sub>3</sub> fumigation the signal recovered again to pre-fumigation levels. The second day of the experiments closely resembled the first day. Again, at certain ozone levels comparable amounts of oxidation products were formed, correlating with similar levels of overall ozone uptake in the plant enclosure. These results are strong indications that the diterpenoid layer at the surface of the emitting tobacco varieties provides long-term protection against ozone, highlighting its relevance.

## 6 Macroscopic model calculations

Similarly to the microscopic fluid dynamic simulations presented in the main text, we performed macroscopic model calculations (see Materials and methods). These show clearly the beneficial effect of ozone surface reactions. In Fig. S3 the ozone concentration isosurfaces are shown, where the ozone concentration is 10% of the concentration in air entering the simulated box. For both the non-reactive (Fig. S3a) and the reactive plant (Fig. S3b), ozone uptake by the leaves under the given flow conditions results in an ozone depleted layer around the plant. Leaves located at the downwind side of the plant are generally exposed to less intense ozone stress. If the leaf surface is reactive (Fig. S3a), the ozone depleted layer is broader. When in real forest environments surface reactive plants grow close to each other, intrinsically unprotected plants growing in between benefit from the reduced ozone concentration, too. This effect could find application in agriculture similar to the push-pull concepts used against biotic stressors (Cook et al., 2007).

## 7 Comparison of stomatal ozone fluxes in the case of non-reactive and reactive leaf surfaces

In the case of a plant having a reactive leaf surface, the stomatal ozone flux is reduced compared to the same plant with an inert leaf surface. This can be shown mathematically. In the following calculations we use the same notation for ozone concentrations and resistances as in Fig. 5a+b in the main text.

In the case of a non-reactive (nr) leaf surface, the stomatal ozone flux  $F_{s,nr}$  equals the total ozone flux  $F_{tot,nr}$  entering the leaf boundary layer:

$$F_{s,nr} = F_{tot,nr} \quad (1)$$

Since ozone entering the stomata has to overcome the boundary layer resistance  $R_{b,nr}$  first, we can write:

$$F_{s,nr} = \frac{c_{b,nr} - c_i}{R_s} = \frac{c_a - c_{b,nr}}{R_{b,nr}} \quad (2)$$

Assuming  $c_i = 0$  (Laisk et al., 1989) we get:

$$c_{b,nr} = \frac{R_s \cdot c_a}{R_s + R_{b,nr}} \implies \quad (3)$$

$$F_{s,nr} = \frac{c_a}{R_s + R_{b,nr}} \quad (4)$$

In the case of a reactive (r) leaf surface, due to the additional surface sink the total ozone flux  $F_{tot,r}$  is split into a stomatal flux  $F_{s,r}$  and a non-stomatal flux component  $F_{ns,r}$ :

$$F_{tot,r} = F_{s,r} + F_{ns,r} \quad (5)$$

Again,  $F_{tot,r}$  has to overcome the boundary layer resistance  $R_{b,r}$  and we can write:

$$\frac{c_a - c_{b,r}}{R_{b,r}} = \frac{c_{b,r} - c_i}{R_s} + \frac{c_{b,r} - c_{c,r}}{R_{sc}} \quad (6)$$

Assuming again  $c_i = 0$  (Laisk et al., 1989) and  $c_{c,r} = 0$  in the case of a very reactive leaf surface with every ozone molecule lost at the surface we get:

$$\frac{c_a - c_{b,r}}{R_{b,r}} = \frac{c_{b,r}}{R_s} + \frac{c_{b,r}}{R_{sc}} \implies \quad (7)$$

$$c_{b,r} = \frac{c_a \cdot R_s \cdot R_{sc}}{R_{b,r} \cdot (R_s + R_{sc}) + R_s \cdot R_{sc}} \implies \quad (8)$$

$$F_{s,r} = \frac{c_a \cdot R_{sc}}{R_{b,r} \cdot (R_s + R_{sc}) + R_s \cdot R_{sc}} \quad (9)$$

Consequently, the fraction of the stomatal fluxes in the case of a reactive and a non reactive leaf surface is:

$$\frac{F_{s,r}}{F_{s,nr}} = \frac{\frac{c_a \cdot R_{sc}}{R_{b,r} \cdot (R_s + R_{sc}) + R_s \cdot R_{sc}}}{\frac{c_a}{R_s + R_{b,nr}}} \quad (10)$$

If we further assume that the boundary layer resistance does not change with the surface reactivity of a leaf ( $R_{b,nr} = R_{b,r} =: R_b$ ), we can simplify:

$$\frac{F_{s,r}}{F_{s,nr}} = \frac{R_{sc} \cdot (R_s + R_b)}{R_b \cdot (R_s + R_{sc}) + R_s \cdot R_{sc}} \quad (11)$$

Eqn. 11 is graphically illustrated in Fig. S4, showing how  $\frac{F_{s,r}}{F_{s,nr}}$  depends on different resistance ratios ( $\frac{R_s}{R_{sc}}$  and  $\frac{R_s}{R_b}$ ). In the case of  $R_{sc} \gg R_s$ , i.e. the leaf surface is inert,  $\frac{F_{s,r}}{F_{s,nr}} \rightarrow 1$ . In the case of a perfectly ozone scavenging leaf surface,  $R_{sc} \ll R_s$  and  $\frac{F_{s,r}}{F_{s,nr}} \rightarrow 0$ , i.e. the stomatal flux  $F_{s,r}$  is much lower than  $F_{s,nr}$ .

Strictly speaking, above calculations are correct only for perfectly inert or perfectly ozone scavenging leaf surfaces. In the case of a semi-reactive leaf surface, these calculations would be considerably more complicated, since in that case the ozone concentration within the leaf boundary layer is varying with the surface parallel distance from the stomata. Therefore different boundary layer concentrations have to be assumed as reference for stomatal and non-stomatal ozone fluxes to the leaf surface. In order to account for these varying boundary layer ozone concentrations, additional resistances have to be introduced (see next section).

## 8 Resistance scheme for ozone depletion on a semi-reactive leaf surface or in the case of non-zero intercellular ozone concentrations

In the main text we showed resistance schemes for ozone depletion on illuminated leaves having a non-reactive (Fig. 5a) and a reactive surface (Fig. 5b). In this respect, reactive means that every ozone molecule hitting the surface is being destroyed, resulting in an ozone concentration of zero at the leaf surface. In nature, however, the surface composition of leaves will always lie some point in between these two extremes: reactive semi-volatile compounds can be deposited on intrinsically non-reactive surfaces and not every ozone molecule hitting a semi-reactive (sr) surface will be destroyed. This situation can be depicted in a slightly more complex resistance scheme as shown in Fig. S5a. When the ozone depletion at the leaf surface is not complete, the ozone concentration in the leaf boundary layer is not equally distributed over the entire leaf surface. The ozone concentration is lowest close to the stomata ( $c_{b,sr}$ ) due to the efficient stomatal sink. At a certain horizontal distance from the stomata, the ozone concentration in the leaf boundary layer ( $c_{b,sr}^*$ ) is higher if the surface is semi- or non-reactive.  $c_{b,sr}^*$  is the reference concentration for the surface chemical resistance  $R_{sc,sr}$ .

The concentration gradient caused by the differences between  $c_{b,sr}$  and  $c_{b,sr}^*$  results in a diffusive ozone transport towards the stomatal pores. This fact is accounted for by introducing an additional resistance  $R_x$ , which limits this surface parallel transport path.

Conversely, in the case of non-zero intercellular ozone concentration (which has been observed e.g. in

experiments applying extremely high ozone concentrations ( $> 1$  ppmv, see Moldau and Bichele (2002)), but perfectly ozone scavenging leaf surface, the ozone concentration would be higher close the stomata and lower at a certain horizontal distance from the stomata. This would result in a diffusive ozone transport away from the stomata, thus eventually further limiting stomatal ozone uptake. In this case the same resistance scheme (Fig. S5a) could be used.

Applying now a Y- $\Delta$  transform (Kennelly, 1899), known from electrical circuits, we get the resistance scheme shown in Fig. S5b. Here,  $R'_x$ ,  $R''_x$  and  $R'_{b,SR}$  can be obtained from  $R_x$ ,  $R_{b,SR}$  and  $R_{b,SR}^*$ .

The stomatal resistance  $R_s$  and  $R'_x$  as well as the surface chemical resistance  $R_{sc,SR}$  and  $R''_x$  could be combined to single resistances  $R'_{s,SR}$  ( $= R_s + R'_x$ ) and  $R'_{sc,SR}$  ( $= R_{sc,SR} + R''_x$ ), respectively. This implicates that the resistance scheme for a semi-reactive surface could be modelled similarly to that of a reactive leaf surface (see Fig. 5b). One should bear in mind though, that in this case  $R'_{s,SR}$  differs from  $R_s$  which is usually obtained from the stomatal conductance of water. To be precise,  $R'_x$  and  $R''_x$  have to be considered whenever there exists a surface parallel ozone gradient in the leaf boundary layer (cf. Fig. 5a), which is the case for semi- and non-reactive leaf surfaces (and stomata not being infinitely close to each other).  $R_x$  and therefore also  $R'_x$  and  $R''_x$  depend strongly on the sink strength of the leaf surface towards ozone. Only in the case of reactive leaf surfaces (cf. Fig. 5b+d) the net surface parallel ozone transport is zero and therefore  $R'_{s,SR} = R_s$ . While the range of  $R'_x$  and  $R''_x$  values is difficult to estimate, we want to point out here that disregarding  $R_{sc,SR}$  will lead to an overestimation of stomatal ozone flux, since  $c_{b,SR}$  strongly depends on the leaf surface sink.

## References

- Altimir, N., Tuovinen, J. P., Vesala, T., Kulmala, M., and Hari, P.: Measurements of ozone removal by Scots pine shoots: Calibration of a stomatal uptake model including the non-stomatal component, *Atmospheric Environment*, 38, 2387–2398, doi:10.1016/j.atmosenv.2003.09.077, 2004.
- Altimir, N., Kolari, P., Tuovinen, J.-P., Vesala, T., Bäck, J., Suni, T., Kulmala, M., and Hari, P.: Foliage surface ozone deposition: a role for surface moisture?, *Biogeosciences*, 3, 209–228, doi:10.5194/bg-3-209-2006, 2006.
- Atkinson, R. and Arey, J.: Atmospheric degradation of volatile organic compounds., *Chemical Reviews*, 103, 4605–4638, doi:10.1021/cr0206420, 2003.
- Cook, S. M., Khan, Z. R., and Pickett, J. A.: The use of push-pull strategies in integrated pest management., *Annual review of entomology*, 52, 375–400, doi:10.1146/annurev.ento.52.110405.091407, 2007.



- Cremer, D.: Theoretical determination of molecular structure and conformation. 7. Stereoselectivity of the ozonolysis reaction, *Journal of the American Chemical Society*, 103, 3619–3626, doi:10.1021/ja00403a001, 1981.
- Criegee, R.: Mechanism of Ozonolysis, *Angewandte Chemie International Edition in English*, 14, 745–752, doi:10.1002/anie.197507451, 1975.
- Epstein, S. A. and Donahue, N. M.: The kinetics of tetramethylethene ozonolysis: decomposition of the primary ozonide and subsequent product formation in the condensed phase., *The journal of physical chemistry. A*, 112, 13 535–13 541, doi:10.1021/jp807682y, 2008.
- Finlayson-Pitts, B. J. and Pitts, J.: *Chemistry of the Upper and Lower Atmosphere*, Elsevier, San Diego, doi:10.1016/B978-012257060, 2000.
- Goldstein, A. H. and Galbally, I. E.: Known and Unexplored Organic Constituents in the Earth's Atmosphere, *Environmental Science & Technology*, 41, 1514–1521, doi:10.1021/es072476p, 2007.
- Hasson, A. S., Chung, M. Y., Kuwata, K. T., Converse, A. D., Krohn, D., and Paulson, S. E.: Reaction of Criegee Intermediates with Water Vapor - An Additional Source of OH Radicals in Alkene Ozonolysis?, *The Journal of Physical Chemistry A*, 107, 6176–6182, doi:10.1021/jp0346007, 2003.
- Jenkin, M. E. and Clemitshaw, K. C.: Ozone and other secondary photochemical pollutants: chemical processes governing their formation in the planetary boundary layer, *Atmospheric Environment*, 34, 2499–2527, doi: 10.1016/S1352-2310(99)00478-1, 2000.
- Kennelly, A.: Equivalence of triangles and three-pointed stars in conducting networks, *Electrical World and Engineer*, 34, 413–414, 1899.
- Kroll, J. H., Sahay, S. R., Anderson, J. G., Demerjian, K. L., and Donahue, N. M.: Mechanism of HO<sub>x</sub> Formation in the Gas-Phase Ozone-Alkene Reaction. 2. Prompt versus Thermal Dissociation of Carbonyl Oxides to Form OH, *The Journal of Physical Chemistry A*, 105, 4446–4457, doi:10.1021/jp004136v, 2001.
- Laisk, A., Kull, O., and Moldau, H.: Ozone Concentration in Leaf Intercellular Air Spaces Is Close to Zero, *Plant Physiology*, 90, 1163–1167, doi:10.1104/pp.90.3.1163, 1989.
- Lamaud, E., Carrara, A., Brunet, Y., Lopez, A., and Druilhet, A.: Ozone fluxes above and within a pine forest canopy in dry and wet conditions, *Atmospheric Environment*, 36, 77–88, doi:10.1016/S1352-2310(01)00468-X, 2002.
- Moldau, H. and Bichele, I.: Plasmalemma protection by the apoplast as assessed from above-zero ozone concentrations in leaf intercellular air spaces, *Planta*, 214, 484–487, doi:10.1007/s00425-001-0678-0, 2002.

Wisthaler, A. and Weschler, C. J.: Reactions of ozone with human skin lipids: sources of carbonyls, dicarbonyls, and hydroxycarbonyls in indoor air., *Proceedings of the National Academy of Sciences of the United States of America*, 107, 6568–75, doi:10.1073/pnas.0904498106, 2010.

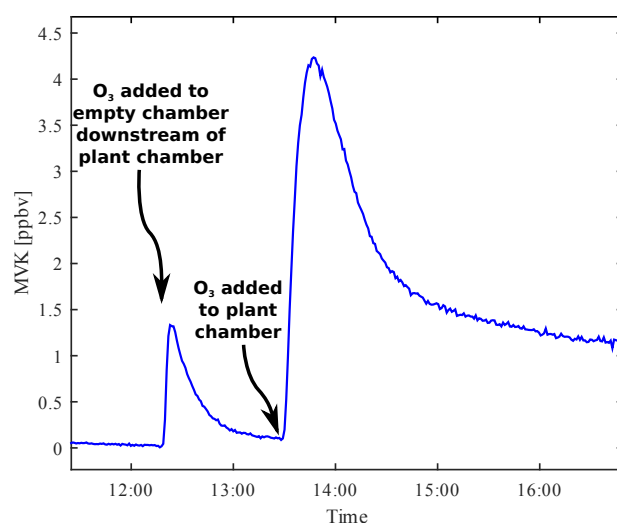


**Figure S1:** Two chamber ozone fumigation experiment with an *Ambalema* variety. The tobacco plant was installed in a plant enclosure, which was connected to a second, empty chamber at the downstream side. When ozone was added to the empty chamber, the MVK signal deriving from surface ozonolysis of semi-volatile *cis*-abienol deposited in the empty chamber decreased quickly. When ozone was added to the plant chamber, the MVK signal approximated a steady state, since the plant surface represented a continuous diterpenoid source. In this steady state, *cis*-abienol ozonolysis occurred prevalingly at the plant surface. For details refer to the text.

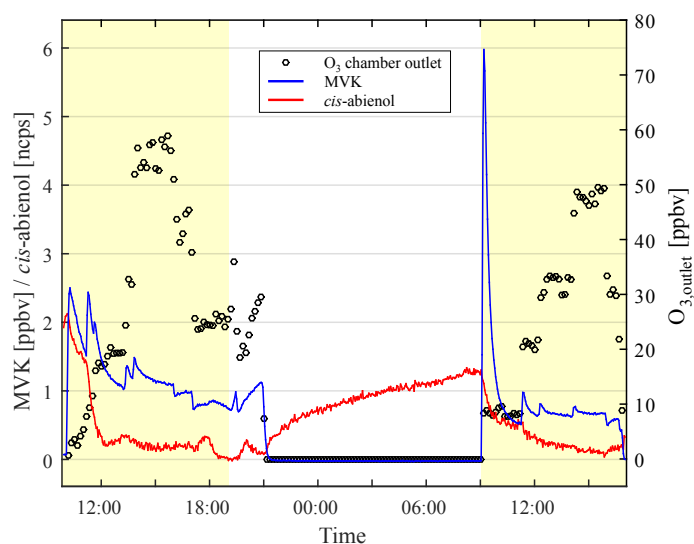


**Figure S2:** Experiment with an *Ambalema* plant simulating diurnal ozone variations. Yellow shaded areas represent times when the plant was illuminated. Addition of ozone resulted in an immediate reduction of the signal of semi-volatile *cis*-abienol and an initial MVK burst, deriving from *cis*-abienol ozonolysis on all surfaces. The *cis*-abienol signal recovered over night, leading to a huge MVK burst from surface ozonolysis at 09:00AM after restarting the ozone fumigation. **Depicted ozone levels were measured at the plant enclosure outlet and are proportional to the total ozone flux.**

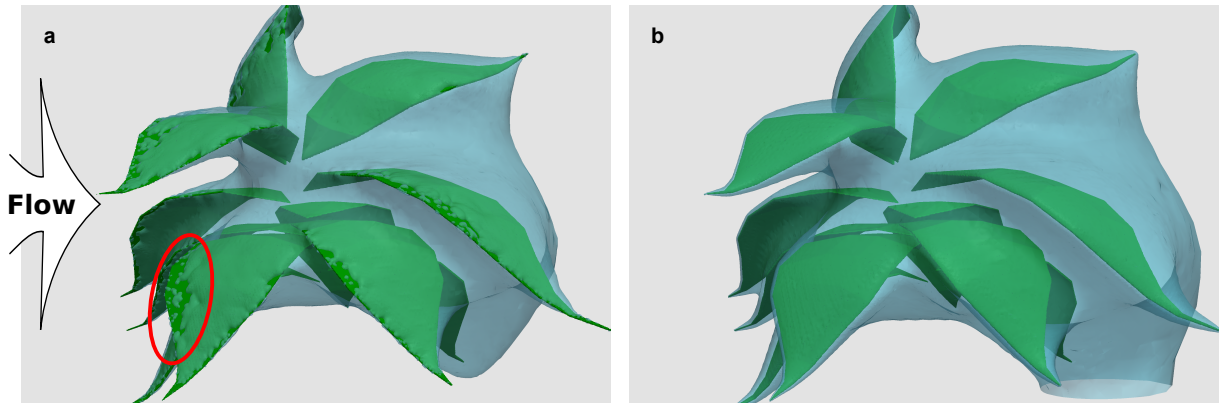


**Figure S3:** Macroscopic fluid dynamic calculations. The plots show the isosurfaces (in light blue color) of equal ozone concentration obtained from model simulations, in which similar plants without (a) or with (b) ozone-reactive leaf surface were fumigated with ozonated air (entering from the left side). The concentration at the isosurfaces corresponds to 10 % of the ozone concentration in the advecting air. In the case of a non-reactive leaf surface (a), solely stomatal uptake is responsible for the reduced ozone concentration in the leaf boundary layer. In places directly exposed to the advecting ozone-rich air, the leaf surface itself is exposed to high ozone concentrations (above the 10 % limit, see e.g. the area indicated by the red ellipse). In contrast, ozonolysis at the plant surface further reduces the ozone concentration in the air layer adjacent to the leaf surface (b). As a result, the reactive leaf surface expands the ozone depleted area. This effect, in combination with the lack of the pore effect for ozone on reactive leaf surfaces, diminishes the amount of phytotoxic ozone entering the leaf stomata.

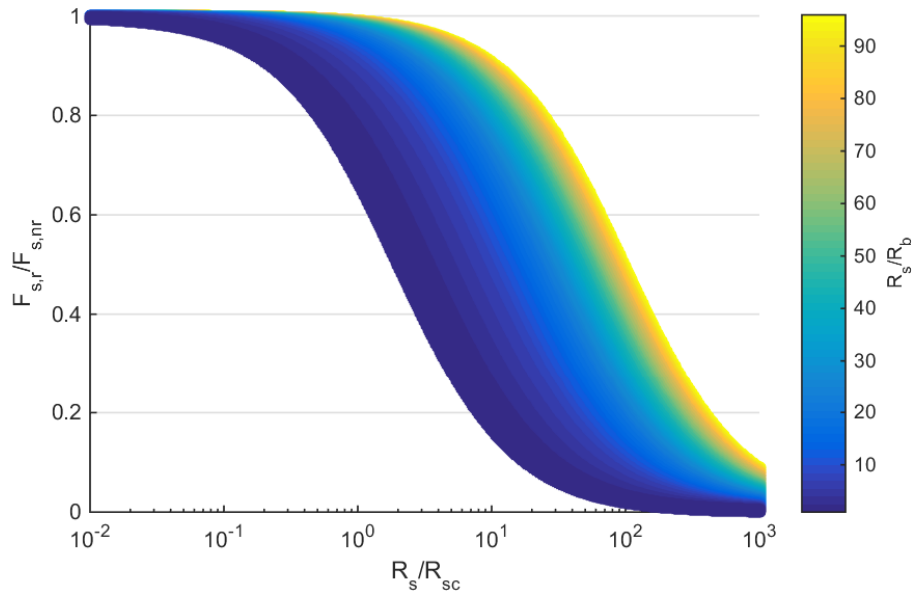


**Figure S4:** Comparison of stomatal ozone fluxes in the case of a non-reactive leaf surface ( $F_{s,nr}$ ) and a reactive leaf surface ( $F_{s,r}$ ). The stomatal ozone flux varies depending on the surface reactivity, which is inversely proportional to the surface chemical resistance  $R_{sc}$ . Moreover, also the boundary layer resistance  $R_b$  influences the stomatal flux.

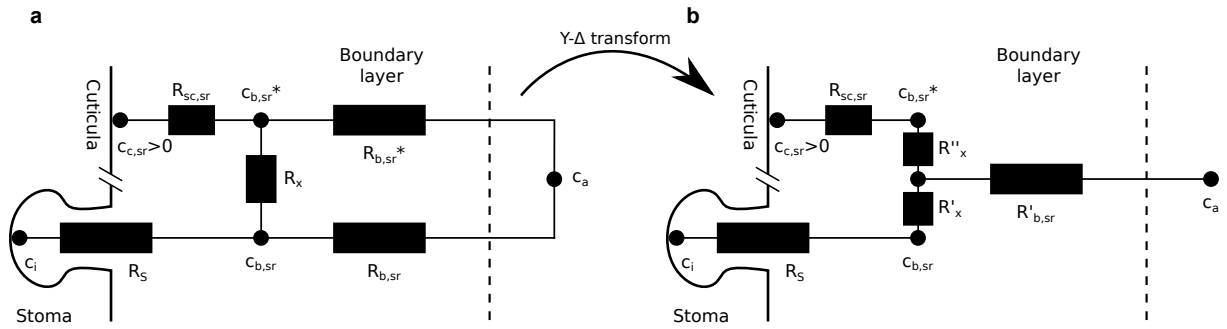


**Figure S5:** Resistance scheme of ozone uptake by a plant leaf with a semi-reactive (sr) surface or in the case of non-zero intercellular ozone concentrations ( $c_i$ ).  $c_c$ ,  $c_b$  and  $c_a$  denote ozone concentrations at the leaf surface, in the boundary layer and in ambient air, respectively.  $R_s$ ,  $R_{sc}$  and  $R_b$  denote the stomatal, surface chemical and boundary layer resistances.  $R_x$  limits the surface parallel ozone transport in the leaf boundary layer from the cuticula towards the stomatal pores. The resistance scheme in **a** can be transformed into that shown in **b** by applying a Y- $\Delta$  transform. For details refer to the text.

**Table S1:** Relative humidities  $RH$  in the plant enclosure during ozone fumigation experiments of different tobacco varieties. Values are given for the same time ranges, for which the total ozone conductance has been calculated (see Fig. 4) and include standard errors of 5 (13), 2 (6), 1 (5) and 3 (5) replicates of *Ambalema*, *Basma Drama*, *BYBA* respectively *3H02* in dark (light) experiments.

Plant variety	RH [%]	
	dark	light
<i>Ambalema</i>	$62 \pm 2$	$78 \pm 2$
<i>Basma Drama</i>	$55 \pm 2$	$79 \pm 4$
<i>BYBA</i>	60	$86 \pm 1$
<i>3H02</i>	$54 \pm 2$	$76 \pm 2$